White Rose Research Online

eprints@whiterose.ac.uk
https://eprints.whiterose.ac.uk
Universities of Leeds, Sheffield and York

Deposited via The University of Sheffield.

White Rose Research Online URL for this paper:
https://eprints.whiterose.ac.uk/id/eprint/247202/

Version: Published Version

Article:
Aryaee, S., Kunz, N., Hosseinzadeh, M. et al. (2026) A bi-objective MILP model for pandemic vaccine allocation and distribution with behavioral adaptation. Journal of Humanitarian Logistics and Supply Chain Management. pp. 1-31. ISSN: 2042-6747

https://doi.org/10.1108/jhlscm-11-2025-0229

Reuse
This article is distributed under the terms of the Creative Commons Attribution (CC BY) licence. This licence allows you to distribute, remix, tweak, and build upon the work, even commercially, as long as you credit the authors for the original work. More information and the full terms of the licence here: https://creativecommons.org/licenses/

Takedown
If you consider content in White Rose Research Online to be in breach of UK law, please notify us by emailing eprints@whiterose.ac.uk including the URL of the record and the reason for the withdrawal request.

UNIVERSITY OF LEEDS
University of Sheffield
UNIVERSITY of York

A bi-objective MILP model for pandemic vaccine allocation and distribution with behavioral adaptation

Sara Aryaee
School of Industrial and Technology Management, College of Management, University of Tehran, Tehran, Iran
Nathan Kunz
Department of Informatics, Faculty of Management, Economics and Social Sciences, University of Fribourg, Fribourg, Switzerland
Mahnaz Hosseinzadeh
Sheffield University Management School, University of Sheffield, Sheffield, UK, and
Mansour Momeni
School of Industrial and Technology Management, College of Management, University of Tehran, Tehran, Iran

Abstract

Purpose – The purpose of this study is to develop a comprehensive optimization framework for pandemic vaccine allocation and distribution that minimizes both distribution costs and disease-induced mortality. The work addresses the need for timely, equitable, and logistically feasible vaccine delivery, particularly in settings with constrained resources and infrastructure.

Design/methodology/approach – A bi-objective, multiproduct, multiperiod mixed-integer linear programming (MILP) model is formulated to integrate inter- and intra-provincial routing, cold chain requirements, vehicle availability and maintenance and vaccine spoilage. The model incorporates a piecewise linear vaccination rate that dynamically adjusts based on prior public acceptance trends. A context-informed, scenario-based application inspired by the COVID-19 vaccination campaign in Iran is presented to illustrate the model's structure and policy-relevant insights, along with sensitivity analyses on vehicle capacity and disease spread rate.

Findings – The model generates distribution and allocation plans that satisfy the modeled cold-chain and fleet constraints and illustrate the tradeoffs between distribution cost, mortality and equity under the assumed epidemiological and behavioral settings. Sensitivity analyses further examine how outcomes vary with transportation capacity and disease spread conditions.

Practical implications – The framework can be adapted to different geographic and epidemiological contexts, guiding ministries of health and humanitarian logistics planners in designing responsive and equitable vaccination strategies.

Originality/value – This study integrates detailed routing, cold chain compatibility, vehicle management and behavioral adaptation into a single optimization framework – features rarely combined in existing literature. It provides policymakers a decision-support modeling framework that has the potential to support pandemic preparedness and response under the modeled assumptions.

Keywords Vaccine allocation, Vaccine distribution, Pandemic logistics, Covid-19, Public acceptance modeling

Paper type Research paper

1. Introduction

The global outbreak of COVID-19 has confirmed the critical significance of efficient and timely immunization campaigns during pandemics. Vaccination campaigns are not only dependent on biomedical adequacy but also on the effectiveness of logistics frameworks that support equitable and timely vaccine distribution. A well-structured vaccine allocation and distribution plan plays a critical role in limiting infection rates, particularly in developing countries with limited health-care foundation and logistical capacity. Past outbreaks of highly infectious diseases, such as Ebola, SARS, MERS and Zika, have similarly demonstrated the widespread disruptions that pandemics can impose (Delivorias and Scholz, 2020; World Health Organization, 2024a, 2024b). As a result, governments and international organizations have increasingly recognized the need to design resilient vaccine supply chains that can minimize mortality while maintaining continuity

The current issue and full text archive of this journal is available on Emerald Insight at: **https://www.emerald.com/insight/2042-6747.htm**

Journal of Humanitarian Logistics and Supply Chain Management
Emerald Publishing Limited [ISSN 2042-6747]
[DOI 10.1108/JHLSCM-11-2025-0229]

© Sara Aryaee, Nathan Kunz, Mahnaz Hosseinzadeh and Mansour Momeni. Published by Emerald Publishing Limited. This article is published under the Creative Commons Attribution (CC BY 4.0) license. Anyone may reproduce, distribute, translate and create derivative works of this article (for both commercial and non-commercial purposes), subject to full attribution to the original publication and authors. The full terms of this license may be seen at http://creativecommons.org/licences/by/4.0/

Received 4 November 2025
Revised 7 April 2026
12 July 2026
Accepted 13 September 2026

Downloaded from www.emerald.com/jhlscm/article-pdf/doi/10.1108/JHLSCM-11-2025-0229/11895066/jhlscm-11-2025-0229en.pdf by University of Sheffield user on 29 October 2026

across critical sectors (Dashraath *et al.*, 2020; Rémy *et al.*, 2015). Nevertheless, persistent global disparities in vaccine access, often driven by uncoordinated distribution and uneven resource availability, highlight the importance of developing robust, data-driven decision-support models to inform both national and international vaccine logistics planning under conditions of scarcity, disruption and demand uncertainty (Goentzel *et al.*, 2023; Rastegar *et al.*, 2021).

In response to these challenges, a considerable body of literature has emerged focusing on mathematical optimization models for vaccine allocation and distribution during epidemics and pandemics. For example, Rastegar *et al.* (2021) developed an inventory-location model to ensure equitable vaccine distribution in resource-constrained environments. Georgiadis and Georgiadis (2021) presented a holistic supply chain framework that integrates production, storage and transportation stages. Smalley *et al.* (2015) demonstrated how hybrid distribution strategies can be used to minimize infection in cholera-endemic regions. Building on these efforts, various researchers have explored more advanced features including bi-level programming for equity and mortality balancing (Valizadeh *et al.*, 2023), integration with AI and machine learning for demand forecasting (Kamran *et al.*, 2023), and robust modeling frameworks that account for system disruptions and uncertainties (Taghipour *et al.*, 2023). Equity concerns have been addressed through fairness-driven allocation models (Balcik *et al.*, 2022; Fadaki *et al.*, 2022; Rastegar *et al.*, 2021), while other studies have extended classical models to capture multiechelon network complexities and cold chain requirements (Khodaee *et al.*, 2022; Kochakkashani *et al.*, 2023; Moadab *et al.*, 2023).

However, our comprehensive review of the literature (see Table 1) reveals several persistent limitations. First, most models treat inter-provincial and intra-provincial logistics separately, leading to fragmented planning. Second, few models incorporate vehicle availability, maintenance and cold chain compatibility constraints, factors that critically influence real-world feasibility. Third, although some recent studies incorporate behavioral dynamics (e.g. social acceptance or trust), these are typically modeled as static or scenario-based inputs rather than adaptive processes that evolve over time. Consequently, there is a need for integrated models that capture logistical, infrastructural and behavioral complexities in a dynamic and scalable manner.

2. Literature review

During the COVID-19 pandemic, an unprecedented amount of research emerged to meet the urgency and scale of global vaccine deployment. Shiri *et al.* (2024) introduced a two-stage vaccine supply chain design integrating machine learning (boosted neural networks) with a fuzzy optimization framework to address lead time and demand uncertainty. Habibi *et al.* (2023) proposed a two-phase optimization approach separating strategic planning (facility location, resource allocation) from tactical execution (inventory, transportation), validated on COVID-19 data.

Other pandemic-specific contributions expanded the modeling scope. Valizadeh *et al.* (2023) offered a bi-level optimization model balancing equity and mortality minimization at the policy level with logistics cost reduction at the operational level. Kamran *et al.* (2023) used a hybrid of system dynamics and artificial intelligence to dynamically optimize demand forecasting and vaccine logistics, emphasizing flexibility and public acceptance. Taghipour *et al.* (2023) presented a robust model integrating uncertainty, disruptions and resource allocation to enhance resilience in vaccine delivery. Sarigol *et al.* (2023) developed a multiobjective optimization model for COVID-19 vaccine order allocation that incorporates substitution between vaccine types, aiming to minimize unvaccinated individuals, vaccination delays and procurement costs under uncertainty. Hegde *et al.* (2023) developed a two-regime queuing framework to analyze COVID-19 vaccine distribution under supply-constrained and hesitancy-constrained regimes, providing insights into how both capacity limitations and public acceptance shape rollout performance.

Broader frameworks emerged to unify supply chain sustainability and responsiveness. Moadab *et al.* (2023) developed a multiobjective MILP model incorporating economic, environmental and social goals under pandemic disruptions, solved with hybrid metaheuristics (NSGA-II and MOPSO). Kochakkashani *et al.* (2023) applied K-means clustering to manage cold/noncold vaccine flows in a four-echelon network. Khodaee *et al.* (2022) introduced deprivation cost minimization through equity-driven humanitarian cold chain distribution.

Several studies emphasized equity. Kar and Jenamani (2025) proposed a multimodal hub-and-spoke vaccine distribution model that incorporates a regional vulnerability index derived from a modified SIR epidemiological model to prioritize hub locations and ensure equitable coverage of high-risk areas. Balcik *et al.* (2022) and Tavana *et al.* (2026) developed mathematical programming models embedding fairness and infrastructure disparities into vaccine allocation. Similarly, Goentzel *et al.* (2023) designed a mixed-integer programming model for vaccine network design to maximize immunization coverage, integrating facility location and allocation decisions, and validated the model through a case study in Gambia in collaboration with UNICEF. Fadaki *et al.* (2022) focused on prioritizing high-risk groups and minimizing infections over multiple periods. Thul and Powell (2023) contributed a stochastic optimization framework to manage allocation uncertainty using real-time data.

Pre-COVID studies also shaped the literature on vaccine allocation and distribution. Enayati and Özaltın (2020) focused on equitable influenza vaccine allocation. Yang *et al.* (2021) and Yang and Rajgopal (2021) used robust two-period frameworks to model vaccine outreach under uncertainty. Smalley *et al.* (2015), Chen *et al.* (2014) and Qasem *et al.* (2020)introduced models tailored to cholera and low-resource settings. Lim *et al.* (2022) and Ribeiro (2016) explored the design of hub-and-spoke cold chain networks.

To provide an overview of the literature on optimization-based studies vaccine allocation and distribution models, a structured literature search was conducted (see most relevant studies in Table 1). Major academic databases, including ScienceDirect, SpringerLink, Emerald Insight and IEEE

Downloaded from www.emerald.com/jhlscm/article-pdf/doi/10.1108/JHLSCM-11-2025-0229/11895066/jhlscm-11-2025-0229en.pdf by University of Sheffield user on 29 October 2026

Downloaded from www.emerald.com/jhlscm/article-pdf/doi/10.1108/JHLSCM-11-2025-0229/11895066/jhlscm-11-2025-0229en.pdf by University of Sheffield user on 29 October 2026

Table 1 Comparison of vaccine allocation and distribution models with respect to modeling approach, operational features and decision-support characteristics

Feature/Study[a]	Tavana *et al.* (2026)	Rastegar *et al.* (2021)	Fadaki *et al.* (2022)	Taghipour et al. (2023)	Kamran *et al.* (2023)	Valizadeh *et al.* (2023)	Goodarzian *et al.* (2022)	This Study
Model type	MILP	MILP	Multiperiod optimization	Robust possibilistic multiobjective optimization	Stochastic multiobjective MILP with system dynamics simulation	Bi-level MILP (robust)	Stochastic multiobjective MILP + system dynamics simulation	Bi-objective MILP
Objective(s)	Max. equity (max–min delivery-to-demand ratio)	Max. equity (max–min delivery-to-demand ratio)	Min. unvaccinated risk	Min. cost, max. route reliability, min. unmet demand	Min. cost, max. equity, max. desirability	Min. mortality risk and inequality (upper level), Min. cost (lower level)	Min. total cost, Max. equity, Max. vaccination desirability	Min. cost and mortality
Cold Chain Management	✓	×	×	×	✓	✓	✓	✓
Multiechelon Network	✓	✓	×	✓	✓	✓	✓	✓
Equity constraints	✓	✓	✓	×	✓	✓	✓	✓
Pandemic-specific features	✓	✓	✓	✓	✓	✓	✓	✓
Uncertainty modeled	×	×	×	✓	✓	✓	✓	×
AI/heuristics used	×	×	×	✓	✓	×	✓	×
Multivaccine types	✓	×	×	✓	✓	✓	✓	✓
Time-phased allocation	✓	✓	✓	✓	✓	✓	✓	✓
Public acceptance dynamics	×	×	×	×	✓	×	✓	✓
Routing/vehicle logistics	✓	×	×	✓	✓	✓	×	✓
Vehicle maintenance/type activation	×	×	×	×	×	×	×	✓
Sensitivity analysis	✓	✓	✓	✓	✓	✓	✓	✓

Note(s): [a]✓ indicates that the corresponding feature is explicitly modeled or incorporated in the study; × indicates that it is not explicitly modeled.
Source(s): Authors' own work

Xplore, were searched using combinations of keywords such as "vaccine allocation," "vaccine distribution," "COVID-19," "optimization model," "MILP," "equitable allocation" and "supply chain." The search focused on peer-reviewed journal articles published in English and included both pre-COVID and COVID-19-era studies.

Studies were screened for relevance to quantitative optimization modeling of vaccine supply chains. Articles that were purely epidemiological, simulation-only without optimization components or unrelated to allocation–distribution decision-making were excluded. After removing duplicates and nonrelevant records, the selected studies were analyzed and compared based on their modeling approach, objective structure, operational features (e.g. cold chain integration, routing, uncertainty) and case study context. The search strategy, inclusion/exclusion criteria and classification dimensions used to compile Table 1 are summarized in Appendix A and Appendix B, which are provided as on-line supplementary material to enhance transparency.

2.1 Synthesis of insights and gaps across research streams

The reviewed literature can be organized into several complementary research streams, each contributing important insights but also leaving specific methodological gaps. A first stream focuses on allocation and prioritization decisions under scarcity, often emphasizing fairness objectives (e.g. equity constraints, proportionality or priority groups). These models provide clear guidance on "who should receive vaccines first" and how to formalize ethical tradeoffs; however, allocation is frequently treated without explicit integration of distribution feasibility, assuming simplified transportation or ignoring vehicle-level constraints. As a result, allocation policies may be optimal on paper yet difficult to operationalize when routing, fleet availability and cold-chain limitations become binding.

A second stream emphasizes distribution and routing (including multiechelon vaccine delivery networks and vehicle-routing formulations). This stream captures the operational reality that transport capacity, travel distance and routing structure strongly shape timely coverage. Recent studies have investigated vaccine distribution using vehicle routing approaches, particularly in the context of last-mile delivery and operational efficiency under capacity and logistical constraints (e.g. Sun *et al.*, 2021). Yet, many routing-focused studies treat vaccine supply, demand satisfaction, and prioritization rules in a simplified manner, and often model inter-regional and intra-regional distribution as separate or sequential problems, which can weaken coordination between national dispatch decisions and local last-mile delivery. Relatedly, a third stream investigates cold-chain and perishability, highlighting that temperature compatibility and spoilage risks are central in vaccine logistics. While these studies provide essential operational realism, cold-chain requirements are commonly represented as fixed feasibility rules rather than being linked to endogenous fleet decisions (e.g. vehicle activation/assignment choices by type) across planning periods.

A fourth stream addresses behavioral dynamics and vaccine acceptance. This stream recognizes that uptake can vary over time due to trust, perceived risk or prior campaign performance, and it highlights the importance of incorporating demand-side uncertainty and feedback into planning. However, behavioral elements are often introduced externally (scenario parameters) or studied separately from detailed logistics constraints, limiting the ability to evaluate how distribution policies and operational constraints interact with evolving acceptance.

Taken together, the literature reveals a persistent gap: existing models often advance specific components of the problem in isolation, while pandemic vaccination campaigns require simultaneous coordination across allocation, multiechelon distribution, cold-chain feasibility and evolving acceptance under resource constraints. This gap motivates the integrated framework proposed in this study, which jointly models inter- and intra-provincial distribution, vehicle-type activation and compatibility, multiperiod vaccine flows and a dynamic acceptance mechanism within a unified bi-objective optimization structure to support scenario-based policy analysis. Building on these identified gaps, the next section formalizes the specific contributions and methodological advancements of the present study.

3. Methodology

This paper develops a bi-objective, multiproduct, multiperiod mixed-integer linear programming (MILP) model for vaccine allocation and distribution during pandemics. The proposed framework is illustrated through a context-informed, scenario-based application inspired by the COVID-19 vaccination context in Iran. The model simultaneously minimizes total distribution costs and disease-induced mortality, operating at both inter-provincial and intra-provincial levels. Key logistical elements such as vehicle routing, maintenance, storage compatibility and vaccine spoilage are explicitly included in the formulation. A distinctive feature of this model is the use of a piecewise linear vaccination rate function that dynamically adjusts based on public acceptance trends observed in previous periods. This mechanism allows the model to capture evolving societal trust and behavioral uptake patterns, which are crucial to real-world vaccination outcomes but rarely embedded in quantitative optimization frameworks.

Compared to existing models, the proposed approach offers several novel contributions. First, it integrates inter- and intra-provincial vehicle routing within a unified supply chain structure, ensuring operational coherence across different geographic scales. Second, the model includes vehicle activation and maintenance logic that aligns with both cost and feasibility considerations. Third, it supports multivaccine allocation with differentiated cold chain constraints and aligns vaccine types with appropriate transportation modes. Fourth, the adaptive vaccination rate provides a realistic approximation of dynamic public acceptance, thereby linking demand-side behavior to supply-side logistics. To the best of our knowledge, this is the first study that comprehensively incorporates these features within a single bi-objective optimization model.

By addressing these research gaps, the model offers a comprehensive decision-support framework for national health authorities and humanitarian logistics planners. The numerical example is informed by structural and publicly available

Downloaded from www.emerald.com/jhlscm/article-pdf/doi/10.1108/JHLSCM-11-2025-0229/11895066/jhlscm-11-2025-0229en.pdf by University of Sheffield user on 29 October 2026

characteristics of the Iranian context, including provincial administrative divisions, population size and age-group distribution, approximate inter-provincial geographic distances and epidemiological parameters consistent with reported COVID-19 mortality ranges. These contextual elements are used to construct a realistic but stylized network representation rather than to replicate historical operational decisions.

The proposed framework is not limited to a specific case such as COVID-19 in Iran and may be adapted to other epidemic and pandemic contexts by modifying demographic, epidemiological and logistical input parameters, thereby providing a basis for strategic vaccination planning and scenario-based analysis. Specifically, the network structure reflects one national distribution center, designated hub provinces, and nonhub provinces consistent with Iran's territorial organization, while cost and epidemiological parameters are calibrated within literature-supported ranges applicable to the national context.

3.1 Model assumptions

The proposed model is based on several key assumptions, including:

- Vaccines are transported to the hub province via air transport.
- Vaccines from the hub provinces are transported overland to nonhub provinces.
- Considering that aerial transportation is not feasible for many provinces, the possibility of vaccine distribution from the distribution center via overland means exists.
- For each province, there is the possibility to use three different types of refrigerated vehicles (Type R1, R2 and R3) and three different types of freezer vehicles (Type F1, F2 and F3), to fulfill the specific vaccine cold chain requirements. These types are abstract representations that differ based on predefined capacity and cost parameters within the model. They are not intended to correspond to specific commercial vehicle models or industry classifications, but rather to simulate the availability of multiple vehicle options with varying logistical characteristics. The numerical values for each type of vehicle, such as transport capacity and acquisition cost, are treated as input parameters. This allows the model to determine which vehicle types to activate and deploy in each province based on optimization of cost and feasibility. Activating a specific type of vehicle is thus a decision variable in the model, enabling flexible fleet selection tailored to the distribution needs of each region.
- There are three types of vaccines with different cold chain requirements. The first type (V1) can only be transported using vehicles equipped with freezers (storage temperature of −15°C or lower, (Objio *et al.*, 2024), while other types of vaccines (V2 and V3) can be transported using vehicles equipped with refrigeration (storage temperature between 2°C and 8°C, Objio *et al.*, 2024).
- A small percentage of the transported vaccines may spoil due to potential uncontrolled storage conditions, with this percentage being accounted for upon arrival at the injection center.
- Given that the disease spread pattern resembles a Poisson distribution (Zhao *et al.*, 2021), and the model is simulated over a 24-week horizon, a truncated segment of the Poisson distribution is used to approximate the disease spread rate, and the dosage for the second dose of the vaccine is considered to be equivalent to the dosage of the first dose.
- Public acceptance of vaccination is represented through a piecewise linear function that adjusts the maximum vaccination rate based on vaccination uptake in previous periods. This formulation captures the behavioral response in a simplified and aggregated manner, without explicitly modeling individual-level decision processes.
- The population is divided into age groups indexed by $g \in G$, which are used in the model to represent aggregated vaccination decisions across different population segments.
- Figure 1 provides a schematic overview of the vaccine distribution from the central distribution center to hub and nonhub provinces.

The vaccine distribution process begins at a central distribution center ($o = 0$), which supplies vaccines to both hub provinces ($u \in U$) and directly to other nonhub provinces ($j \in J$). Each province consists of multiple interior regions ($z \in Z$), with $z = 0$ representing the provincial center where vaccines arrive and $z \neq 0$ representing subregions that receive vaccines via intra-provincial transport. Hub provinces not only serve their own regions but also distribute vaccines to other provinces. Transport from the central distribution center to hub provinces may occur via air, while inter-provincial and intra-provincial deliveries are conducted via land. Each vaccine type is transported using a specific class of vehicle based on its temperature requirement (e.g. V1 with freezer vehicles, V2 and V3 with refrigerated vehicles). Vehicle selection affects cost through the fixed cost of acquiring each vehicle type V, FCost.

These modeling assumptions reflect structural characteristics commonly observed in centrally coordinated pandemic vaccination programs. Centralized allocation decisions represent typical national emergency command structures. Fleet constraints capture physical vehicle availability limitations. Cold-chain compatibility requirements are consistent with global public health vaccine storage standards. The behavioral adaptation component reflects documented risk-perception dynamics influencing vaccination uptake. These assumptions are not country-specific; rather, they represent general structural features of centrally coordinated vaccination strategies and can be adapted to other national or international contexts.

3.2 Model formulation

This section describes our model formulation, with all sets, parameters and decision variables presented in Table 2.

3.3 Mathematical model

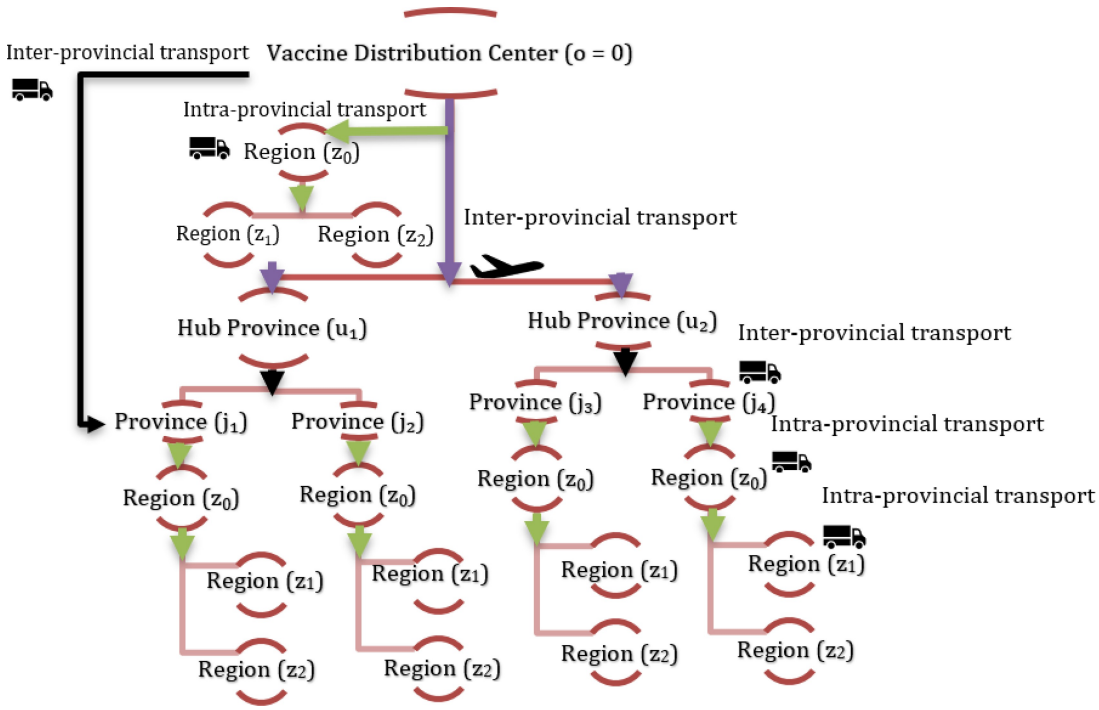
This section presents the mathematical model for an optimal vaccine allocation and distribution network during a viral disease outbreak. The proposed model, described by equations (1)–(60), aims to minimize total costs while simultaneously reducing the number of deaths.

3.3.1 Objective function 1: minimize the following costs

- Cost of purchasing vehicles required for inter-provincial transportation network.

Downloaded from www.emerald.com/jhlscm/article-pdf/doi/10.1108/JHLSCM-11-2025-0229/11895066/jhlscm-11-2025-0229en.pdf by University of Sheffield user on 29 October 2026

Figure 1 Schematic overview of vaccine distribution network



Source: Authors' own work

- Cost of purchasing vehicles required for intra-provincial transportation network.
- Cost of vaccine transportation in inter-provincial transportation network.
- Cost of vaccine transportation in intra-provincial transportation network.
- Cost of vaccines sent from the distribution center to hub provinces via air transport.
- Cost of vaccines sent from the distribution center to nonhub provinces via land transport.
- Cost of vaccines sent from the distribution center to interior regions of the distribution center:

$$
\begin{aligned}
z_1 = \min & \sum_{j\in\{U\cup O\}}\sum_{v\in V} FCost_v^1 R_{jv}^1 + \sum_{j\in N}\sum_{v\in V} FCost_v^2 R_{jv}^2 \\
& + \sum_{l\in\{U\cup O\}}\sum_{i\in N}\sum_{j\in N}\sum_{m\in l_M}\sum_{t\in T} CPK^1 Ecost_m R_{jv}^1 Dist_{ij} p_{lijt}^m \\
& + \sum_{l\in N}\sum_{z\in\{0\}}\sum_{f\in Z}\sum_{m\in l_{M2}}\sum_{t\in T} CPK^2 Ecost_m R_{jv}^2 Dist_{jzf} q_{jzft}^m \\
& + \sum_{u\in U}\sum_{v\in V}\sum_{t\in T} Cost_v Pallet_v x_{uvt}^o \\
& + \sum_{o\in O}\sum_{j\in N}\sum_{v\in V}\sum_{m\in O_M}\sum_{t\in T} Cost_v Pallet_v y_{ojvt}^m \\
& + \sum_{o\in O}\sum_{z\in\{0\}}\sum_{m\in O_{M2}}\sum_{t\in T} Cost_v Pallet_v yz_{ozvt}^m \qquad (1)
\end{aligned}
$$

3.3.2 Objective function 2: minimize the number of deaths

$$z_2 = \min \sum_{j\in N}\sum_{z\in Z}\sum_{g\in G}\sum_{t\in T} d_{zgt}^j \qquad (2)$$

3.3.3 Constraints

Vehicles are explicitly differentiated by type in the model and are not treated as identical units. The index m represents distinct vehicle types characterized by different capacities, acquisition costs and cold-chain compatibility. Vehicle activation is modeled through binary decision variables, and capacity constraints are enforced at the vehicle type level. This formulation allows the optimization model to endogenously select appropriate vehicle types based on logistical requirements and vaccine storage conditions.

The mathematical constraints are organized according to the main operational components of the proposed vaccine distribution system. They represent inventory and capacity management, transportation and routing decisions, vehicle activation, cold-chain compatibility, vaccination dynamics and equity considerations within a unified optimization framework. This organization facilitates interpretation of the mathematical formulation and clarifies the role of each group of constraints.

The amount of vaccines type V1 (requiring a freezer) sent to hub provinces in each period should not exceed the storage

Downloaded from www.emerald.com/jhlscm/article-pdf/doi/10.1108/JHLSCM-11-2025-0229/11895066/jhlscm-11-2025-0229en.pdf by University of Sheffield user on 29 October 2026

Table 2 Nomenclature

Symbol	Description
Index sets	
$i, j, l \in N = \{1, 2, \ldots, N\}$	The set of all provinces. Indices *i* and *j* are used to denote origin and destination provinces. Index l represents the vehicle base node (either the distribution center or a hub province) from which inter-provincial routes are initiated
$o \in O = \{1\} \subseteq N$	Vaccine distribution center (subset of provinces in *N*)
$u \in U \subseteq N$	Hub provinces (subset of provinces in *N* used as intermediate distribution nodes)
$v \in V = \{1, 2, 3\}$	Type of vaccine. Vaccine type $v = 1$ requires freezer conditions, while $v = 2,3$ require refrigeration
$m \in j_M = \{j_1, j_2, \ldots, j_m\} \mid j \in \{U \cup O\}$	Index *m* refers to available vehicles of different types. Sets J_m and J_{m2} distinguish vehicles used in inter-provincial and intra-provincial transportation, respectively
$m \in j_{M2} = \{j_1, j_2, \ldots, j_{m2}\} \mid j \in N$	Index *m* refers to available vehicles of different types. Sets J_m and J_{m2} distinguish vehicles used in inter-provincial and intra-provincial transportation, respectively
$t \in T = \{1, 2, \ldots, T\}$	The period (weeks)
$z \in Z = \{0, 1, 2, \ldots, Z\}$	The interior regions within each province, used to model intra-provincial distribution
$g \in G = \{1, 2, \ldots, G\}$	Age groups
Parameters	
CPK^1	Transportation cost per kilometer for inter-provincial vaccine distribution, reflecting longer travel distances and higher operational intensity between provinces
CPK^2	Transportation cost per kilometer for intra-provincial vaccine distribution, reflecting shorter travel distances and localized routing within provinces
Cap_t^R	The capacity of the central refrigerated hub province for each period
Cap_t^F	The capacity of the central freezer hub province for each period
Node	The number of nonhub provinces and provinces other than the distribution center
Cap_{jm}^{Vac}	The capacity of vehicle "*m*" (where m corresponds to a specific vehicle type – either freezer-equipped or refrigerated, with capacity levels Type 1, Type 2 or Type 3) for transporting vaccines inter-provincial from province "*j.*"
$Cap_{jm}^{Vac\prime}$	The capacity of vehicle "*m*" for transporting vaccines intra-provincial "*j.*"
$FCost_v^1$	The fixed cost of acquiring vehicle required to transport vaccine type *v* in the inter-provincial transportation network
$FCost_v^2$	The fixed cost of acquiring vehicle required to transport vaccine type *v* in the intra-provincial transportation network
$Ecost_m$	The coefficient of difference in cost between refrigerated vehicles and freezer-equipped vehicles
$Pallet_v$	The number of vaccines of type "*v*" available on each pallet
$Cost_v$	The total cost of vaccine type "*v*"
Ds_t	The disease spread rate during period *t*, which represents a cut of the Poisson function within the selected time cut
$Pop_{zg}^{\prime j}$	The population of age group "*g*" in region "*z*" of province "*j.*"
α	The case-fatality rate (mortality rate among infected/affected individuals)
$VehType_{mv}$	The binary parameter indicating which type of vaccine should be transported by which type of vehicle
$Rate_v$	The vaccine spoilage rate
Dr_g^j	Disease prevalence rate (or infection exposure rate) for age group *g* in province *j.*
Variables	
x_{uvt}^o	The amount of vaccine type "*v*" sent from distribution center "*o*" to hub province "*u*" in period "*t*" via air transport
p_{ijlt}^m	Binary variable equal to 1 if vehicle type "*m,*" assigned to departure node l (distribution center or hub province), travels from province "*i*" to province "*j*" in period "*t*"; 0 otherwise
H_{lit}^m	An auxiliary variable to prevent the formation of sub-tours for vehicles "*m*" dispatched from center "*l*" passing through node "*i*" in period "*t.*"
y_{jivt}^m	The amount of vaccine type "*v*" sent from center "*j*" (either a distribution center or hub provinces) to province "*i*" via vehicle "*m*" in period "*t.*"
q_{jzft}^m	If vehicle "*m*" travels between two regions "*z*" and "*f*" intra-provincial "*j*" in period "*t*", it equals 1; otherwise, it equals 0
K_{jzt}^m	An auxiliary variable to prevent the formation of sub-tours for vehicles "*m*" in province "*j*" passing through region "*z.*"

(***continued***)

Downloaded from www.emerald.com/jhlscm/article-pdf/doi/10.1108/JHLSCM-11-2025-0229/11895066/jhlscm-11-2025-0229en.pdf by University of Sheffield user on 29 October 2026

Table 2

Symbol	Description
yz^{m}_{jzvt}	The amount of vaccine type "v" sent from province "j" to region "z" via vehicle "m" in period "t."
$R^{1}_{jm} \mid j \in \{U \cup O\}$	If the designated vehicle "m" is purchased and used in the inter-provincial transportation network for cities in the set O and U, it equals 1; otherwise, it equals 0
$R^{2}_{jm} \mid j \in N$	If the anticipated vehicle "m" is purchased and used in the intra-provincial transportation network for city "j," it equals 1; otherwise, it equals 0
$zz^{1}_{jzgt}, zz^{2}_{jzgt}, zz^{3}_{jzgt}$	Auxiliary binary variables used to control incremental increases in the minimum vaccination rate for second doses. These variables are activated when the uptake of first doses in previous periods increases by 5%, 10% or 15%, respectively. They allow the model to dynamically adjust second-dose coverage based on recent public response trends
$Vac^{Dose1}_{jzgt2}, Vac^{Dose2}_{jzgt2}$	The respective amounts of the first and second doses of vaccine type "v" administered in province "j," region "z" and age group "g" in period "t."
F^{Dose2}_{jzgt}	The cumulative amount of vaccine type "v" second doses administered in province "j," region "z" and age group "g" up to period "t."
D^{j}_{zgt}	The number of deaths in province "j," region "z" and age group "g" during period "t."
d^{j}_{zgt}	Auxiliary non-negative variable used to approximate the real-valued death estimate while preserving model linearity

Source(s): Authors' own work

capacity of that type of vaccine at the vaccine distribution center:

$$\sum_{u\in U}\sum_{v\in\{1\}} x^{o}_{uvt} \le Cap^{F}_{t} \qquad \forall\ t \in T \tag{3}$$

The total amount vaccines type V2 and V3 (requiring refrigeration) sent to the hub provinces in each period should not exceed the storage capacity of that type of vaccine in the vaccine distribution center:

$$\sum_{u\in U}\sum_{v\in v\ \{1\}} x^{o}_{\mathrm{uvt}} \le Cap^{R}_{t} \qquad \forall\ t \in T \tag{4}$$

In each period "t", all provinces except for the hub provinces and the distribution center must be serviced by at least one of the vehicles dispatched from the distribution center or hub provinces:

$$\sum_{i\in U\cup O}\sum_{m\in j_M}\sum_{j\in N} p^{m}_{ijlt} \le 1 \qquad \forall l \in N\ \{U\cup O\},\ t \in T \tag{5}$$

In each period t, for each vehicle m and origin node i (distribution center or hub province), the binary routing variable ensures that vehicle m can be assigned to at most one destination j. This constraint prevents a single vehicle from being simultaneously allocated to multiple inter-provincial routes within the same period:

$$\sum_{l\in N} p^{m}_{ijlt} \le 1 \qquad \forall m \in i_M, i \in \{U\cup O\}, j \in N \tag{6}$$

This constraint is used to prevent the formation of sub-tours in the inter-provincial network:

$$H^{m}_{lit} - H^{m}_{ljt} + Node{*}p^{m}_{lijt} \le Node - 1\ \ \forall m \in l_M, l \in \{U\cup O\}, i, j \in N\ \{U\cup O\},\ \ t \in T \tag{7}$$

The magnitude of incoming and outgoing vehicles in each period for each node must be equal, where the node represents the count of nonhub provinces and hubs provinces:

$$\sum_{i\in N} p^{m}_{lijt} = \sum_{i\in N} p^{m}_{ljit} \qquad \forall m \in l_M, l \in \{U\cup O\}, j \in N,\ \ t \in T \tag{8}$$

For nonhub province "i" in each period, the number of incoming vehicles dispatched from hub province "l" shall be limited to a maximum of one vehicle:

$$\sum_{l\in\{U\cup O\}}\sum_{m\in l_M}\sum_{j\in N} p^{m}_{ljit} \le 1 \qquad \forall i \in N\ \{U\cup O\}, t \in T \tag{9}$$

All vehicle activation and sequencing constraints are defined separately for each vehicle type m, as indicated by the index set on the right-hand side of the corresponding constraints. Accordingly, these constraints are enforced individually for each vehicle type and are not applied in an aggregated manner. In light of the potential availability of multiple vehicles, to preserve the sequence of used vehicles, the subsequent constraint necessitates the model to activate the vehicles sequentially within the inter-provincial transportation network. For instance, instead of activating vehicles numbered 1 and 3, vehicles numbered 1 and 2 should be activated. This constraint does not affect the solution of the problem and merely aids in the formal selection of vehicles, preserving their sequential order:

Downloaded from www.emerald.com/jhlscm/article-pdf/doi/10.1108/JHLSCM-11-2025-0229/11895066/jhlscm-11-2025-0229en.pdf by University of Sheffield user on 29 October 2026

$$BigM\sum_{i\in N}\sum_{\mathcal{J}\in N\ \{U\cup O\}} p^m_{lijt} \geq \sum_{i\in N}\sum_{\mathcal{J}\in N\ \{U\cup O\}} p^{m+1}_{lijt}\ \ \forall l\in\{U\cup O\},\ m\in l_M,\ \ t\in T \tag{10}$$

If vehicle m is purchased and used within the inter-provincial transportation network for province j, the variable R^1_{lm} will take a value of 1:

$$\sum_{i\in N}\sum_{j\in N}\sum_{t\in T} p^m_{lijt} \leq BigM*R^1_{lm} \quad \forall\ l\in\{U\cup O\}, m\in l_M \tag{11}$$

If vehicle m is purchased and used within the intra-provincial transportation network for province j, the variable R^2_{jm} will take a value of 1:

$$\sum_{z\in Z}\sum_{f\in Z}\sum_{t\in T} q^m_{jzft} \leq BigM*R^2_{jm}\ \ \forall\ j\in N, m\in j_{M2} \tag{12}$$

The total sum of all vaccines transferred from hub province j using vehicle m available at this hub province in each period shall not exceed the capacity of the vehicle:

$$\sum_{v\in V}\sum_{i\in N\ \{U\cup O\}} y^m_{jivt} \leq Cap^{Vac}_{jm}\ \ \forall m\in j_M, j\in\{U\cup O\},\ \ t\in T \tag{13}$$

Vaccines are dispatched from hub province u to province i using vehicle m, available at hub u in period t if vehicle m enters that province:

$$\sum_{v\in V} y^m_{uivt} \leq BigM\sum_{j\in N\ O} p^m_{ujit}\ \ \forall\ u\in U, m\in u_M, i\in N\ \{U\cup O\},\ \ t\in T \tag{14}$$

Vaccines are dispatched from distribution center o to province i using vehicle m, available in period t if vehicle m enters that province:

$$\sum_{v\in V} y^m_{oivt} \leq BigM\sum_{j\in N\ U} p^m_{ojit}\ \ \forall\ o\in O, m\in o_M, i\in N\ \{U\cup O\},\ \ t\in T \tag{15}$$

In each period t, for each province j, all interior regions z of that province must be serviced by one of the available vehicles m at the region $z=0$ of province j:

$$\sum_{m\in j_{M2}}\sum_{f\in Z} q^m_{jzft} = 1\ \ \forall j\in N, z\in Z,\ \ t\in T \tag{16}$$

The incoming flow to each region z from each province j in each period t must be equal to the outgoing flow from that region within the same province and the same time period:

$$\sum_{f\in Z} q^m_{jzft} = \sum_{f\in Z} q^m_{jfzt}\ \ \forall m\in j_{M2}, j\in N, z\in Z,\ \ t\in T \tag{17}$$

This constraint is used to prevent the formation of sub-tours within the intra-provincial network:

$$K^m_{jzt} - K^m_{jft} + |Z-\{0\}|*q^m_{jzft} \leq |Z-\{0\}| - 1\ \ \forall m\in j_{M2},\ j\in N, f, z\in Z,\ \ t\in T \tag{18}$$

For centers z other than the vaccine distribution center $\{0\}$ in each period t, the number of incoming vehicles dispatched from the region $z=0$ of province j shall be at most one vehicle. This restriction limits routing/dispatch decisions; shipped quantities are still governed by vehicle capacity constraints, and demand is not forced to be fully satisfied within a single period:

$$\sum_{f\in Z}\sum_{m\in j_{M2}} q^m_{jfzt} \leq 1 \quad \forall j\in N, z\in Z\{0\}, t\in T \tag{19}$$

Similar to what was explained regarding the inter-provincial transportation network, here as well, given the potential availability of multiple vehicles, to preserve the sequence of used vehicles, the subsequent constraint necessitates the model to activate the vehicles sequentially within the intra-provincial transportation network:

$$BigM\sum_{f\in Z}\sum_{z\in Z\ \{0\}} q^m_{jzft} \geq \sum_{f\in Z}\sum_{z\in Z\ \{0\}} q^{m+1}_{jzft}\ \ \forall j\in N, m\in j_{M2},\ \ t\in T \tag{20}$$

In each period t, the total sum of all vaccines transported from the region $z=0$ of province j using vehicle m available at province j to use in the intra-provincial transportation network shall not exceed the capacity of the vehicle:

$$\sum_{v\in V}\sum_{z\in Z} yz^m_{jzvt} \leq Cap^{Vac}_{jm}{}'\ \ \forall m\in j_{M2}, j\in N,\ \ t\in T \tag{21}$$

Vaccines are dispatched from the distribution center of province j to region z using vehicle m available at that center, which is allocated to that province to use in the intra-provincial transportation network in period t if the vehicle m enters that region:

$$\sum_{v\in V} yz^m_{jzvt} \leq BigM\sum_{f\in Z} q^m_{jfzt}\ \ \forall\ j\in N, m\in j_{M2}, z\in Z\ \{0\}, t\in T \tag{22}$$

In each period t, the total sum of vaccines of type v dispatched by all available vehicles m at each hub province u to other provinces must not exceed the vaccines received at that warehouse from distribution center o:

$$\sum_{m\in u_M}\sum_{i\in N\ \{U\cup O\}} y^m_{uivt} \leq x^o_{uvt}\ \ \forall v\in V, u\in U,\ \ t\in T \tag{23}$$

In each period t, the total sum of vaccines of the first vaccine type (i.e. V1, which requires a freezer) dispatched by all available vehicles m at distribution center o to interior regions z of that center must not exceed the storage capacity of the first type minus the amount sent from that type to other hub province (by air) and other nonhub provinces (by land):

Downloaded from www.emerald.com/jhlscm/article-pdf/doi/10.1108/JHLSCM-11-2025-0229/11895066/jhlscm-11-2025-0229en.pdf by University of Sheffield user on 29 October 2026

$$\sum_{m\in o_{M2}} yz^{m}_{ozvt} \le Cap^{F}_{t} - \sum_{u\in U} x^{o}_{uvt} - \sum_{m\in o_{M}} \sum_{i\in N\ \{U\cup O\}} y^{m}_{oivt} \ \forall v \in \{1\},$$
$$o \in O, z \in \{0\},\ t \in T \tag{24}$$

In each time period t, the total sum of vaccines of the second and third vaccine types (i.e. V2 and V3, which require a refrigerator) dispatched by all available vehicles m at distribution center o to interior regions z of that center must not exceed the storage capacity of the second and third types minus the amount sent from those types to other hub provinces (by air) and other nonhub provinces (by land):

$$\sum_{m\in o_{M2}} yz^{m}_{ozvt} \le Cap^{R}_{t} - \sum_{u\in U} x^{o}_{uvt} - \sum_{m\in o_{M}} \sum_{i\in N\ \{U\cup O\}} y^{m}_{oivt} \ \forall v \in \{2,3\}, o \in O, z \in \{0\},\ t \in T \tag{25}$$

For provinces acting as hubs in the network, considering their capability to cover other provinces besides fulfilling their internal needs after receiving vaccines, in each time period t, the total sum of vaccines dispatched by all available vehicles m at the hub province u to interior regions z of that province must be equal to the number of vaccines received by that province minus the vaccines sent to other provinces:

$$\sum_{m\in u_{M2}} yz^{m}_{uzvt} = \sum_{u\in U} x^{o}_{uvt} - \sum_{m\in u_{M}} \sum_{i\in N\ \{U\cup O\}} y^{m}_{ujvt} \ \forall v \in V, u \in U,$$
$$z \in \{0\},\ t \in T \tag{26}$$

For provinces j other than distribution center and hub provinces, considering these provinces solely consume vaccines in the network and only receive vaccines, therefore, in each period t, the total sum of vaccines dispatched by all available vehicles m to the distribution center of province j ($z = 0$) must be equal to the number of vaccines received by that province:

$$\sum_{m\in u_{M2}} yz^{m}_{jzvt} = \sum_{m\in u_{M}} \sum_{i\in N\ \{U\cup O\}} y^{m}_{ijvt} \ \forall v \in V, j \in N\ \{U \cup O\},$$
$$z \in \{0\},\ t \in T \tag{27}$$

In each period t, the total amount of vaccines dispatched by all available vehicles at the region $z = 0$ of province j. From that center to all regions z within that province must be equal to the number of vaccines available at the distribution center of that province:

$$\sum_{m\in j_{M2}} \sum_{f\in Z\ \{0\}} yz^{m}_{ufvt} = \sum_{j\in u_{M2}} yz^{m}_{jzvt} \ \forall v \in V, j \in N, z \in \{0\},\ t \in T \tag{28}$$

In each period t, the total sum of first and second vaccine doses administered to the population of age group g in region z of province j should not exceed the total quantity of vaccines supplied to that region from the distribution center ($z = 0$), after deduction of the percentage of vaccine spoilage.

Considering the spoilage coefficient of the vaccine, which results in a decimal number of usable doses, and because the number of administered vaccines must be an integer, the model approximates the integer part of the unspoiled supply using a pair of linear inequalities. These inequalities, described in Constraints 30 and 31, ensure that the integer variable representing administered doses lies within one unit of the actual usable amount. This approach avoids nonlinear functions and preserves the model's linear structure:

$$Vac^{Dose1}_{jzgt} + Vac^{Dose2}_{jzgt} = \left| \sum_{m\in j_{M2}} \sum_{f\in Z\ \{0\}} (1 - Rate_{v}) yz^{m}_{ufvt} \right| \ \forall v \in V,$$
$$j \in N, z \in \{0\},\ t \in T \tag{29}$$

Because right-hand side of the constraint, the number of usable vaccines after spoilage, is a decimal value, and the number of administered vaccines must be an integer, we introduce an auxiliary integer variable (denoted here as w for explanation purposes) to approximate the floor of that value.

To preserve linearity, we use the fact that the integer part of any positive decimal number x lies between $x - 1$ and x. Therefore, we apply the following constraints:

$$w \le x$$

$$w \ge x - 1$$

This allows the model to ensure consistency between integer vaccine administration and available (spoilage-adjusted) supply, without using nonlinear floor functions:

$$Vac^{Dose1}_{jzgt} + Vac^{Dose2}_{jzgt} \le \sum_{m\in j_{M2}} \sum_{f\in Z\ \{0\}} (1 - Rate_{v}) yz^{m}_{ufvt} \ \forall v \in V,$$
$$j \in N, z \in \{0\},\ t \in T \tag{30}$$

$$Vac^{Dose1}_{jzgt} + Vac^{Dose2}_{jzgt} \ge \sum_{m\in j_{M2}} \sum_{f\in Z\ \{0\}} (1 - Rate_{v}) yz^{m}_{ufvt} - 1 \ \forall v \in V, j \in N, z \in \{0\},\ t \in T \tag{31}$$

In each period t, the number of first-dose vaccinations administered to age group g in region z of province j is constrained by a time-dependent upper limit that reflects both baseline vaccination capacity and dynamic changes in public acceptance.

Specifically, the vaccination capacity limit in period t is adjusted through a piecewise-linear behavioral adaptation mechanism based on the level of first-dose vaccinations administered in the previous periods. Higher prior vaccination levels allow bounded increases in the vaccination capacity limit for the current period by 1%, 3% or 5%, depending on which behavioral-adaptation condition is satisfied. This formulation captures positive behavioral reinforcement while keeping the model linear and tractable.

These percentage-based adjustments are modeling assumptions designed to reflect the positive feedback effect commonly observed in public health campaigns, where higher uptake in one period can generate more public trust and logistical readiness in the next (Bauch and Galvani, 2013). This piecewise-linear structure enables behavioral

Downloaded from www.emerald.com/jhlscm/article-pdf/doi/10.1108/JHLSCM-11-2025-0229/11895066/jhlscm-11-2025-0229en.pdf by University of Sheffield user on 29 October 2026

responsiveness in the model while keeping the formulation linear and tractable:

$$Vac_{jzgt}^{Dose1} \leq \left(1 + \frac{5 - zz_{jzgt}^{1} - 2zz_{jzgt}^{2} - 2zz_{jzgt}^{3}}{100}\right) Ds_t Pop_{zg}^{j}$$
$$\forall j \in N, z \{0\} \in Z, g \in G, \ t \in T \quad (32)$$

Because assigning a value of 0 to these binary variables relaxes the corresponding vaccination-capacity upper bound without directly requiring additional vaccine administration, the optimization can select 0 whenever the associated behavioral-adaptation condition is satisfied. Therefore, the auxiliary binary variables zz_{jzgt}^{1}, zz_{jzgt}^{2} and zz_{jzgt}^{3} are used only to activate or deactivate the corresponding behavioral-adaptation levels. The Big-M constraints determine whether each adaptation level is admissible according to the vaccination conditions achieved in previous periods. When a behavioral-adaptation condition is satisfied, the corresponding binary variable may take the value 0, allowing the associated increase in vaccination capacity. Otherwise, it is forced to 1, preventing that capacity increase:

$$0.85FVac_{jzg(t-1)}^{Dose1} - Vac_{jzg(t-2)}^{Dose1} \geq -BigM*zz_{jzgt}^{3} \ \forall j \in N,$$
$$z \in Z \{0\}, g \in G, \ t \in T \quad (33)$$

Individuals receiving the first vaccine dose must wait at least 4 weeks before receiving the second dose. Therefore, the number of individuals in age group g in region z of province j receiving the second vaccine dose in one period is at most equal to the number of individuals who received the first vaccine dose four periods ago:

$$Vac_{jzgt}^{Dose2} \leq Vac_{jzg(t-4)}^{Dose1} \ j \in N, z \in Z \{0\}, g \in G, \ t \in T \quad (34)$$

The amount of vaccine administered to the third age group ($g = 3$) in region z of province j during the first four periods must be at least four times the amount of vaccine administered to the remaining age groups in that region. This constraint is imposed to prioritize this age group and offer increased protection to economically active populations (for example age range 30–55 years) compared to younger and older age groups. The value 4 is used as a modeling assumption to enforce strong prioritization of this group in the early phase of the vaccination campaign. It does not reflect actual population ratios and is not based on demographic data. The specific age range of group 3 is illustrative and does not imply a recommended or universally applicable age-based vaccination policy. Remaining age groups ($g = 1, 2, 4, \ldots, G$) are not subject to explicit prioritization constraints and are intentionally treated generically within the model formulation and are not associated with specific numerical age ranges. Additional age-based prioritization can be considered in future work:

$$\sum_{t \leq 4} \sum_{g \in \{3\}} Vac_{jzgt}^{Dose1} \geq 4* \sum_{t \leq 4} \sum_{g \in G\{3\}} Vac_{jzgt}^{Dose1} \ \forall \ j \in N, z \in Z \{0\} \quad (35)$$

According to published studies, the completion rate of second-dose COVID-19 vaccines has reached over 93% in some scenarios, implying a dropout of less than 7% (Shahparvari *et al.*, 2022). In our model, to ensure robustness under low-adherence conditions, the number of individuals in age group g receiving the second vaccine dose in region z of province j in period t is constrained to be at least 70% of the number vaccinated in the relevant prior period.

Specifically, this constraint requires that the number of individuals in age group g receiving the second dose in region z of province j in period t must not be less than 70% of the individuals who received the first dose in the same group and region four periods earlier (i.e. period $t - 4$):

$$Vac_{jzgt}^{Dose2} \geq 0.7*Vac_{jzg(t-4)}^{Dose1} \ \forall \ j \in N, z \in Z \{0\}, g \in G, t \in T,$$
$$t \geq 5 \quad (36)$$

Considering the public interest in receiving the first vaccine dose, if the number of first-dose vaccinations administered in period $t - 1$ increases by at least 5% compared to period $t - 2$, then the minimum number of individuals from age group g in region z of province j who receive the second dose in period t is increased to 80% of those who received the second dose in period $t - 1$.

The 5% threshold refers to a weekly increase, not a daily one. This condition is used to model improved public responsiveness and operational readiness following rising demand.

The 80% value is a modeling assumption intended to simulate a positive behavioral response in second-dose uptake when public interest in vaccination increases. This threshold is not derived from empirical data but can be adjusted if needed to reflect real-world behavioral dynamics or country-specific conditions:

$$Vac_{jzgt}^{Dose2} \geq 0.8*Vac_{jzg(t-1)}^{Dose2} - BigMzz_{jzgt}^{1} \ \forall \ j \in N, z \in Z \{0\},$$
$$g \in G, t \in T \quad (37)$$

Furthermore, if there is a 10% increase in the administration of the first vaccine dose compared to the preceding period, the minimum number of individuals from age group g in region z of province j receiving the second vaccine dose can also be increased to 90% of the number of individuals who received the second dose in the period before that:

$$Vac_{jzgt}^{Dose2} \geq 0.9*Vac_{jzg(t-1)}^{Dose2} - BigMzz_{jzgt}^{2} \ \forall \ j \in N, z \in Z \{0\},$$
$$g \in G, t \in T \quad (38)$$

The variable F_{jzgt}^{Dose2} calculates the cumulative number of individuals from age group g in region z of province j who have received the second vaccine dose up to period t:

$$F_{jzgt}^{Dose2} = \sum_{t2 \leq t} Vac_{jzgt2}^{Dose2} \ j \in N, z \in Z \{0\}, g \in G, \ t \in T \quad (39)$$

The number of deaths in age group g in region z of province j during period t is modeled as the mortality rate applied to an effective at-risk population in that period. The term in parentheses in Constraint (40) represents this at-risk population after excluding individuals who died in prior periods and accounting for the protective effect of full vaccination

Downloaded from www.emerald.com/jhlscm/article-pdf/doi/10.1108/JHLSCM-11-2025-0229/11895066/jhlscm-11-2025-0229en.pdf by University of Sheffield user on 29 October 2026

through a proportional mortality-risk reduction parameter (0.9). Based on published studies, two-dose COVID-19 vaccination substantially reduces the risk of severe disease and death, often exceeding 85%–90% effectiveness (Andrews *et al.*, 2022; Cohn *et al.*, 2022). In line with this evidence, vaccinated individuals enter the effective at-risk population with a proportionally reduced contribution to mortality, implemented through the mortality-reduction parameter applied to the cumulative number of fully vaccinated individuals whose protective effect is assumed to be active within the modeled period.

This formulation provides a tractable linear approximation that incorporates the mortality-reducing effect of full vaccination within the aggregated modeling structure adopted in this study, without explicitly modeling detailed epidemiological dynamics. Dimensional consistency is preserved because all quantities inside the parentheses are population stocks, while the mortality rate converts the resulting stock into period-specific death flows.

Here, D^{j}_{zgt} represents a period-specific death count (flow), while the term inside parentheses represents an effective at-risk population stock; multiplying by α and D^{j}_{r} converts the stock into deaths per period. The disease prevalence rate is assumed homogeneous across regions within each province and depends only on age group g and province j. This simplifying assumption is consistent with the aggregated regional modeling structure adopted in this study:

$$D^{j}_{zgt} = \alpha * Dr^{j}_{g}\left(Pop^{'j}_{zgt} - \sum_{t'<t} D^{j}_{zgt'} - 0.9 * F^{Dose2}_{jzg(t-1)}\right)\ j \in N,\ z \in Z\ \{0\}, g \in G,\ t \in T \tag{40}$$

In the current formulation, the variable d^{j}_{zgt} is constrained to be greater than or equal to D^{j}_{zgt}, which acts as a conservative upper-bound approximation of the real-valued mortality rate. While this does not reflect the exact floor value, it preserves linearity and ensures that mortality estimates remain safe and nonunderestimated. The constraint can be refined in future versions to improve accuracy if needed:

$$d^{j}_{zgt} \geq D^{j}_{zgt}\ j \in N, z \in Z\ \{0\}, g \in G\ t \in T \tag{41}$$

Given that optimization solvers solve problems technically and may not understand some constraints of the real world, it is necessary to express these constraints and prohibitions in mathematical terms. For example, in the real world, practically, it is not possible to allocate a vehicle available in one province to another province. However, because the solver aims at optimizing the objective, it may not recognize these prohibitions. Another example is that in the real world, while it may technically be possible for a vehicle to exit a province and reenter it, such a routing pattern is unrealistic or inefficient in the context of our vaccine distribution model. Therefore, to avoid sub-tours and redundant travel, these loops are explicitly prohibited in the model. Accordingly, the possibility for any vehicle to leave a node (province) and return to the same node within a period is explicitly prohibited in the model:

$$p^{m}_{jiit} = 0\ \forall\ j, i \in N\ ,\ m \in j_M, t \in T \tag{42}$$

The first index of variable p^{m}_{lijt} indicates the origin of the movement of vehicle m. Because ground shipments to provinces are only possible from hub provinces, no node other than a hub province can be the origin of vehicle movements:

$$p^{m}_{lijt} = 0\ \forall\ l \in N\ \{U \cup O\}, i, j \in N\ ,\ m \in l_M, t \in T \tag{43}$$

No vehicle is allowed to travel between hub provinces:

$$p^{m}_{lijt} = 0\ \forall\ l \in N, i, j \in \{U \cup O\}\ ,\ m \in l_M, t \in T \tag{44}$$

Vehicles dispatched from one hub province are not permitted to pass through other hub provinces or return to another hub province:

$$p^{m}_{uijt} = 0\ \forall\ u \in U, i \in N, j \in O\ ,\ m \in l_M, t \in T \tag{45}$$

$$p^{m}_{ujit} = 0\ \forall\ u \in U, i \in N, j \in O\ ,\ m \in u_M, t \in T \tag{46}$$

$$p^{m}_{ujit} = 0\ \forall\ u \in U, i \in U\ and\ i \neq u, j \in N\ ,\ m \in u_M, t \in T \tag{47}$$

$$p^{m}_{uijt} = 0\ \forall\ u \in U, i \in U\ and\ i \neq u, j \in N\ ,\ m \in u_M, t \in T \tag{48}$$

$$p^{m}_{oiut} = 0\ \forall\ o \in O, i \in N, u \in U\ ,\ m \in o_M, t \in T \tag{49}$$

$$p^{m}_{ouit} = 0\ \forall\ o \in O, i \in N, u \in U\ ,\ m \in o_M, t \in T \tag{50}$$

It is not possible to dispatch vehicles other than those available in each hub province:

$$p^{m}_{lijt} = 0\ \forall\ l \in \{U \cup O\}, i, j \in N, m \notin l_M, t \in T \tag{51}$$

It is not possible for any vehicle dispatched from the region $z = 0$ of province j to leave a point and return to the same point in any period:

$$q^{m}_{jzzt} = 0\ \forall\ j \in N\ , z \in Z,\ m \in j_{M2}, t \in T \tag{52}$$

It is not possible to dispatch vehicles other than those available at the region $z = 0$ of province j:

$$q^{m}_{jzft} = 0\ \forall\ l \in \{U \cup O\}, f, z \in Z_{\jmath}\ m \notin j_{M2}, t \in T \tag{53}$$

The transfer of vaccines between hub provinces is not possible:

$$y^{m}_{ijvt} = 0\ \forall\ i, j \in \{U \cup O\},\ v \in V,\ m \in i_M, t \in T \tag{54}$$

It is important to emphasize that Constraints (42) – (54), which restrict inter-hub movements, prohibit cross-hub routing, and limit vehicle departures per period, are policy-driven modeling assumptions rather than universal transportation rules. These constraints reflect a centrally coordinated emergency logistics structure commonly adopted during early outbreak phases or

Downloaded from www.emerald.com/jhlscm/article-pdf/doi/10.1108/JHLSCM-11-2025-0229/11895066/jhlscm-11-2025-0229en.pdf by University of Sheffield user on 29 October 2026

under limited fleet availability, where transportation decisions are tightly regulated to reduce congestion, coordination complexity and operational uncertainty.

These restrictions enhance model tractability and allow clearer interpretation of allocation–routing interactions. However, the proposed framework is sufficiently general and can accommodate more flexible transportation policies by relaxing or modifying these constraints in future extensions without altering the core allocation–distribution structure.

Each type of vaccine must be transported using vehicles compatible with its temperature requirements. Specifically, vaccines of type V1, which require freezing conditions ($T < 15^{\circ}C$), must be transported using freezer-equipped vehicles, while vaccines of type V2 and V3, which require refrigeration ($T = 2^{\circ}C$ –$8^{\circ}C$), must be transported using refrigerated vehicles. Accordingly, the model prohibits the use of any vehicle whose equipment does not match the required cold chain specification of the vaccine being transported:

$$y^{m}_{ijvt} = 0 \ \forall \ i,j \in N, \ \ m \in i_M, \ \ v \in V, VehType_{mv} = 0, t \in T \tag{55}$$

$$yz^{m}_{jzvt} = 0 \ \forall \ j \in N, \ \ z \in Z, m \in j_{M2}, \ \ v \in V, VehType_{mv} = 0, \ \ t \in T \tag{56}$$

In the set Z, which defines the subregions within each province, the index $z = 0$ refers to the provincial distribution center, typically located in the provincial capital. This node functions solely as a logistics point for receiving and dispatching vaccines to other subregions and is not associated with a residential population or vaccine administration.

Therefore, no mortality is calculated for this index:

$$d^{j}_{zgt} = 0 \ \forall \ j \in N, \ \ z \in \{0\}, \ \ g \in G, t \in T \tag{57}$$

While the above constraints may seem obvious, failing to enforce them could lead the solver to obtain misleading results.

The constraint related to the type of variables used in the problem:

$$q^{m}_{ijzt}, p^{m}_{ljit}, zz^{1}_{jzgt}, zz^{2}_{jzgt}, zz^{3}_{jzgt} \in \{0,1\} \tag{58}$$

$$x^{o}_{uvt}, y^{m}_{jivt}, yz^{m}_{jfvt}, Vac^{Dose1}_{jzgt}, Vac^{Dose2}_{jzgt}, \ \ d^{j}_{zgt} \in \mathbb{Z}^{+} \tag{59}$$

$$D^{j}_{zgt}, H^{m}_{it}, K^{m}_{jzt}, F^{Dose2}_{jzgt} \geq 0 \tag{60}$$

3.4 Multiobjective optimization

Multiobjective optimization involves simultaneously optimizing multiple conflicting objectives, making it a challenging task across various domains such as engineering, finance and supply chain management, among others. Contrary to traditional single-objective optimization, multiobjective optimization aims to find a set of solutions that represent a tradeoff among conflicting objectives. One of the well-known methods in the field of multiobjective optimization problem-solving is the Goal Programming model, which was first introduced by Charnes and colleagues (Charnes *et al.*, 1955). In this model, the aim is to minimize the sum of deviations of the problem objectives from predetermined targets. Various versions of the initial form introduced by Charnes and colleagues have been presented to date, each catering to different decision-maker perspectives (Ho, 2019). One of the developments proposed on the basic Goal Programming optimization model is attributed to Lin's research (Lin, 2004). One of these aspects involves normalizing the objective functions, which ensures that the relative importance of objectives measured on different scales is treated equally. In addition, in this model, it is possible to incorporate the relative importance of objectives from the perspective of experts by assigning weights to the objectives. In this research, considering that one objective pertains to cost while the other relates to the number of fatalities, incorporating net deviations in the model biases the attention weights toward the cost function. Indeed, because the cost minimization objective is on a larger scale than the fatality minimization objective, deviations in cost are substantially greater than deviations in the number of fatalities. Consequently, the model will unintentionally tend toward optimizing the cost objective, and the fatality minimization objective will be accorded much less importance. Therefore, to equalize the value of objectives in this problem, the model proposed by Lin will be used (Model 1):

$$\max \lambda \tag{61}$$

$$w_i \lambda \leq \mu_i(x) \tag{62}$$

$$x \in \Omega \tag{63}$$

In which Ω represents the feasible space of the primary problem, w_i denotes the relative importance weight of the ith objective function from the experts' perspective, satisfying $\sum w_i = 1$, and $\mu_i(x)$ is the characteristic function (fuzzy objectives) of the ith objective function, calculated based on the definitions provided by Bellman and Zadeh (1970) as follows:

$$\mu_i(x) = \begin{cases} 1 & f_i(x) < L_i(x) \\ \dfrac{U_i(x) - f_i(x)}{U_i(x) - L_i(x)} & L_i(x) \leq f_i(x) \leq U_i(x) \\ 0 & f_i(x) > L_i(x) \end{cases} \tag{64}$$

where $U_i(x)$ and $L_i(x)$ are, respectively, the upper and lower bounds of the i-th objective function. In this research, the Pay-off Table method has been used to determine the upper and lower bounds of the problem's objective functions. In this approach, objectives are initially solved separately, and with the obtained value for each objective, the problem optimizes the next objective while keeping the achieved objective constant. This process leads to the generation of the following matrix, referred to as the payoff or return table (Table 3) (Isermann and Steuer, 1988):

In this payoff table, the diagonal cells ($z_1{}^1$ and $z_2{}^2$) represent the optimal values of each objective function when optimized individually. The off-diagonal cells ($z_1{}^2$ and $z_2{}^1$) show the value

Downloaded from www.emerald.com/jhlscm/article-pdf/doi/10.1108/JHLSCM-11-2025-0229/11895066/jhlscm-11-2025-0229en.pdf by University of Sheffield user on 29 October 2026

Table 3 The payoff table for the bi-objective optimization model (cost minimization and mortality reduction)

Objective/Bound	The first objective	The second objective
The first objective	z_1^1	z_2^1
The second objective	z_1^2	z_2^2
$L_i(x)$	min $\{z_1^1, z_1^2\}$	min $\{z_2^1, z_2^2\}$
$U_i(x)$	max $\{z_1^1, z_1^2\}$	max$\{z_2^1, z_2^2\}$

Source(s): Authors' own work

of one objective when the other is fixed at its optimum. This matrix structure illustrates the tradeoff relationship between cost minimization and mortality reduction in the bi-objective model.

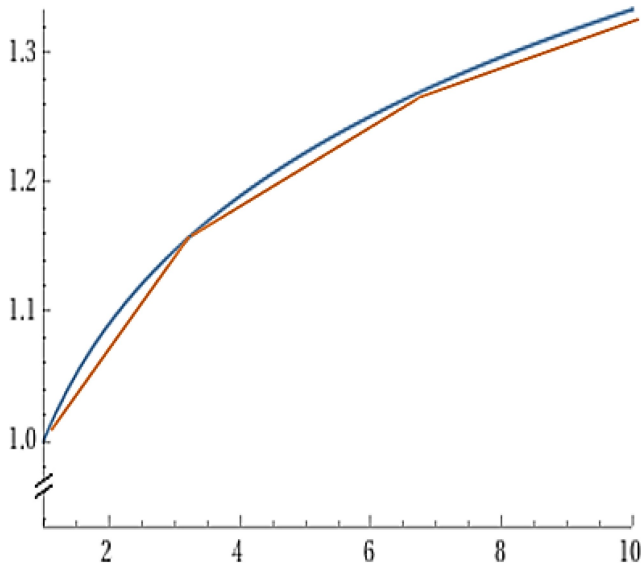
To make the tradeoff between the two objectives more transparent, an additional objective-weight analysis was conducted. After obtaining the lower and upper bounds of the two objective functions using the payoff table, the model was solved under five alternative decision-maker preference structures: $(w_1, w_2) = (0.90, 0.10)$, $(0.70, 0.30)$, $(0.50, 0.50)$, $(0.30, 0.70)$ and $(0.10, 0.90)$, where w_1 denotes the relative importance assigned to distribution cost minimization and w_2 denotes the relative importance assigned to mortality reduction. The balanced case $(0.50, 0.50)$ is used as the baseline scenario. All other input parameters and constraints were held constant across the five runs, allowing the effect of decision-maker preferences on cost, fatalities, vaccine allocation and vehicle activation patterns to be isolated.

3.5 Modeling public acceptance of vaccination

Subsequently, the approach to modeling public acceptance of vaccination in each period will be explained. It is considered as a piecewise linear function to prevent the model from becoming nonlinear. In the process of administering a pandemic vaccine, various factors significantly influence public acceptance. Among the most important of these factors are safety and side effects, efficacy, trust in vaccine-providing institutions, personal experience with the disease (AlJamaan *et al.*, 2022; Roy *et al.*, 2022), among others. Considering each of these factors individually would complicate the modeling process. Moreover, it would be challenging to assume a linear relationship between these factors and public acceptance of vaccination. Among the factors mentioned in the current modeling, an attempt has been made to incorporate the trust factor in the vaccination rate for each period. In this research, trust in vaccine-providing institutions is considered as the vaccination rate in the previous period. To avoid nonlinearizing the problem, a piecewise linear relationship has been used for this purpose (Figure 2 illustrates the relationship between a piecewise linear approximation and a linear function).

In this model, public acceptance is considered as follows: The maximum vaccination rate in each period t will increase by 1% if the vaccination rate in the previous period exceeds 85% of the rate two periods ago, by 3% if the previous period's vaccination rate exceeds 90% of the rate two periods ago and by 5% if the previous period's vaccination rate exceeds 95% of the rate two periods ago. In this way, maintaining or increasing the number of vaccinations in the previous period compared to two

Figure 2 Relationship between a piecewise linear approximation and a linear function



Source: Authors' own work

periods ago will encourage more people to get vaccinated in the current period.

It is important to note that these threshold values (85%, 90% and 95%) and the corresponding step increases (1%, 3% and 5%) used in the piecewise-linear public acceptance formulation are modeling assumptions rather than empirically calibrated parameters. These values are introduced to provide a transparent and tractable representation of positive behavioral feedback observed in vaccination campaigns, where higher uptake in earlier periods can improve public trust, operational readiness and subsequent participation (Bauch and Galvani, 2013; Roy *et al.*, 2022).

The thresholds are structured in a monotonic and bounded manner, ensuring that higher prior uptake leads only to gradual relaxations of vaccination capacity limits. Importantly, these thresholds define upper bounds on vaccination rates and do not force discrete jumps in actual vaccination decisions. The realized vaccination levels remain endogenously determined by supply availability, transportation capacity, routing constraints and the mortality minimization objective.

Empirical evidence from large-scale international surveys indicates substantial cross-country variation in COVID-19 vaccine acceptance and willingness, with some countries reporting high acceptance levels above 80% and, in specific contexts, approaching or exceeding 85%–90%, alongside others below 60% (de Figueiredo and Larson, 2021; Lazarus *et al.*, 2021; Sallam *et al.*, 2022; Solís Arce *et al.*, 2021). These findings document clustering of acceptance in high-coverage regimes, which motivates representing potential positive behavioral reinforcement, such as increased trust, perceived safety and social normalization, through bounded threshold levels in the model.

Accordingly, the selected thresholds (85%, 90% and 95%) are designed to represent transitions between high, very high

Downloaded from www.emerald.com/jhlscm/article-pdf/doi/10.1108/JHLSCM-11-2025-0229/11895066/jhlscm-11-2025-0229en.pdf by University of Sheffield user on 29 October 2026

and near-saturation acceptance regimes reported in empirical studies. The associated step increases (1%, 3% and 5%) are intentionally conservative relative to observed cross-period variations in vaccine uptake, ensuring gradual and bounded behavioral reinforcement rather than abrupt structural shifts.

The numerical results indicate that the main qualitative insights, such as early prioritization of high-risk groups and the tradeoff between cost and mortality, remain structurally robust under the proposed behavioral formulation. While alternative acceptance thresholds could be explored in further analyses, the bounded and monotonic structure adopted here ensures that the core allocation and distribution dynamics are primarily governed by logistical and epidemiological constraints rather than by finely tuned behavioral parameters.

3.6 Numerical example

To demonstrate the application of the proposed model, a numerical example is constructed using a combination of publicly available data and representative estimates. The data set integrates demographic, epidemiological, logistical and economic information to reflect realistic structural characteristics of a national vaccination campaign while maintaining computational tractability. This approach is consistent with humanitarian and pandemic logistics contexts, where detailed operational data are often incomplete, delayed or confidential.

This study uses a data set comprising empirically observed data, literature-calibrated estimates, standards-guided calibrated scenario inputs and structured modeling assumptions. Empirically observed inputs include the number of provinces, population distribution, age-group structure and approximate inter-provincial distances. Literature-calibrated inputs include transportation cost parameters, mortality-related epidemiological parameters and vaccine procurement-cost magnitudes. Standards-guided calibrated inputs include cold-chain storage capacities, vehicle-capacity assumptions, vaccine–vehicle compatibility, pallet-level shipment quantities and spoilage/wastage rates, which are specified using WHO/UNICEF vaccine logistics and cold-chain guidance where exact operational data are not publicly available. Finally, some parameters, such as behavioral adaptation thresholds and selected scenario-based cost multipliers, are retained as transparent modeling assumptions. Table 4 reports the value or range used in the study, the source, the source type and the calibration logic for each main parameter. This classification distinguishes directly observed parameters from calibrated estimates and illustrative modeling assumptions, thereby improving transparency and reproducibility under limited data availability.

Where parameters are expressed in storage volume rather than number of doses, the model converts storage or transport capacity into dose capacity using vaccine-specific packed-volume and shipment-unit assumptions.

3.6.1 *Demographic data.*

Population and administrative data were treated as empirically observed inputs. The number of provinces and the territorial structure of the case study were based on Iran's administrative divisions, while population data were obtained from publicly accessible census and demographic statistics from the Statistical Center of Iran. City- and province-level population data were used to represent the geographic distribution of demand. The population was then divided into age groups to support age-based vaccination and mortality calculations.

Where detailed subregional or age-specific breakdowns were unavailable, proportional estimates were generated from available demographic information to ensure representational balance across regions and age groups. This approach preserves the relative scale and geographic distribution of demand, enabling the model to capture realistic allocation challenges without requiring granular microlevel data that are rarely accessible in emergency settings.

3.6.2 *Epidemiological data*

Epidemiological parameters, including the case-fatality rate (α) and age-specific disease prevalence (Dr_g^j), were aligned with published COVID-19 studies (e.g. Fadaki *et al.*, 2022; Hasan *et al.*, 2021), ensuring consistency with globally documented infection and mortality patterns. Following global evidence, the case-fatality rate (CFR) of COVID-19 among confirmed cases declined during 2020 and stabilized around approximately 2% by the end of the year (Hasan *et al.*, 2021). It should be noted that the CFR differs conceptually from the infection fatality rate (IFR), as CFR reflects only laboratory-confirmed cases and is typically higher than IFR estimates derived from population-based seroprevalence studies.

Large-scale seroprevalence-based systematic evaluations have estimated the global average IFR to lie approximately within the range of 0.1%–0.4%, depending on demographic structure, health-care capacity and geographic context (Ioannidis, 2020; Meyerowitz-Katz and Merone, 2020). These studies document substantial cross-country heterogeneity while consistently indicating that population-level mortality risk is markedly lower than early case-based estimates suggested. In the present study, a population-level mortality parameter of 0.2% is adopted for modeling purposes. This value lies within the empirically documented IFR range reported in the aforementioned meta-analyses and therefore represents a conservative and structurally realistic assumption rather than an extreme scenario. The assumed infection proportion corresponds to a moderate epidemic exposure level consistent with seroprevalence findings reported in multiple national and regional surveys during the first pandemic waves (Ioannidis, 2021).

The disease spread parameter (Ds_t) was represented using a truncated Poisson-type pattern over the 24-week planning horizon, following the modeling assumption that epidemic intensity varies over time rather than remaining constant. This parameter is not intended to reproduce the exact historical trajectory of COVID-19 in Iran. Instead, it provides a tractable time-dependent epidemic-pressure profile that allows the optimization model to evaluate vaccine allocation decisions under evolving disease-spread conditions. The age-specific disease prevalence parameter.

$\left(Dr_g^j\right)$ was calibrated using COVID-19 epidemiological studies and global evidence, while the mortality parameter (α) was aligned with published CFR/IFR evidence. Together, these assumptions allow the model to generate structurally realistic epidemic outcomes without requiring complete real-time epidemiological data sets.

Downloaded from www.emerald.com/jhlscm/article-pdf/doi/10.1108/JHLSCM-11-2025-0229/11895066/jhlscm-11-2025-0229en.pdf by University of Sheffield user on 29 October 2026

Table 4 Data sources and parameter calibration ranges

Parameter	Value/range used in this study	Source	Source type	Calibration/justification
CPK^1	0.5–0.8 US$/km	Goentzel *et al*. (2023)	Literature-calibrated	Goentzel *et al*. (2023) report a representative vehicle operating cost of 0.6 US$/km in a vaccine distribution network case study. In this study, CPK^1 is calibrated around this reported magnitude and specified as 0.5–0.8 US$/km to reflect uncertainty in inter-provincial transportation costs and contextual variability in longer-distance vaccine distribution
CPK^2	0.3–0.5 US$/km	Structured assumption consistent with CPK^1 scaling	Structured modeling assumption	Specified as a structured modeling assumption at approximately 60–70% of CPK^1 to reflect shorter routing distances, reduced fuel consumption, and lower logistical intensity within provinces
Cap_t^R	10, 30 or 40 m^3 refrigerated walk-in cold-room capacity, converted to dose capacity using WHO vaccine-volume calculation procedures	World Health Organization (2017), UNICEF Supply Division (2020), United Nations Children's Fund (UNICEF) (2024)	Standards-guided calibrated scenario input	Refrigerated hub storage capacity is treated as a scenario input, but its magnitude is calibrated using WHO/UNICEF cold-chain capacity guidance and standard walk-in cold-room sizes. UNICEF guidance identifies walk-in cold rooms as key storage infrastructure usually used at central/national level and lists standard cold-room sizes of 10 m^3, 30 m^3 and 40 m^3. The Iran-specific UNICEF report also confirms that Iran's Ministry of Health conducted a national cold-chain assessment and prioritized medical universities/districts for walk-in cold-room installation. Therefore, Cap_t^R is not assumed arbitrarily; it is a standards-guided capacity parameter representing feasible refrigerated storage at a central or hub facility
Cap_t^F	15–20 m^3 freezer-room capacity, or 15 m^3 freezer compartment in a combined 40 m^3 cold/freezer room, converted to dose capacity using WHO vaccine-volume calculation procedures	World Health Organization (2017), (UNICEF Supply Division (2020)	Standards-guided calibrated scenario input	Freezer hub storage capacity is treated as a scenario input, but its magnitude is calibrated using WHO/UNICEF guidance on vaccine storage-capacity calculation and UNICEF standard walk-in freezer-room configurations. UNICEF guidance lists freezer-room options such as a 20 m^3 walk-in freezer and a combined 40 m^3 unit with 25 m^3 cold-room and 15 m^3 freezer-room capacity. Therefore, Cap_t^F represents a realistic freezer-capacity scenario rather than a purely arbitrary assumption. Exact empirical freezer capacity for the Iranian central/hub facilities was not publicly available, so the parameter is transparently classified as a standards-guided calibrated scenario input
Node	Number of provinces	Statistical left of Iran (2026)	Empirically observed	The number of provinces and their administrative structures correspond to the actual territorial divisions used in the case study

(***continued***)

Downloaded from www.emerald.com/jhlscm/article-pdf/doi/10.1108/JHLSCM-11-2025-0229/11895066/jhlscm-11-2025-0229en.pdf by University of Sheffield user on 29 October 2026

Table 4

Parameter	Value/range used in this study	Source	Source type	Calibration/justification
Cap_{jm}^{Vac}	Net usable vehicle capacity = 0.67 × gross vehicle cargo volume; implemented as small/medium/large inter-provincial vehicle-type capacities	World Health Organization (2026), World Health Organization (2017)	Standards-guided calibrated scenario input	The inter-provincial vehicle-capacity parameter is treated as a scenario input because the model uses abstract vehicle types rather than named commercial vehicles. However, the magnitude of the capacity levels is calibrated using WHO guidance on refrigerated vehicles and cold-chain capacity planning. WHO identifies refrigerated vans, trucks and semitrailers as appropriate vaccine-transport equipment and recommends calculating net usable vehicle capacity from gross cargo volume using a utilization factor of 0.67. Therefore, Cap_{jm}^{Vac} represents a standards-guided vehicle-capacity scenario rather than an arbitrary assumption
$Cap_{jm}^{Vac'}$	Smaller vehicle/cold-box-based capacity levels for intra-provincial transport, calibrated from UNICEF/WHO cold-box and vaccine-carrier guidance	World Health Organization (2026), UNICEF Supply Division (2021)	Standards-guided calibrated scenario input	The intra-provincial vehicle-capacity parameter is specified as a smaller scenario capacity than inter-provincial transport, reflecting last-mile or subregional distribution. UNICEF guidance explains that cold boxes are used to transport vaccines from one vaccine store to another and from vaccine stores to health facilities, with typical cold-box capacity between 5 and 25 l, while vaccine carriers hold approximately 0.8–3.4 l. Thus, $Cap_{jm}^{Vac'}$ is calibrated to reflect smaller local delivery units and is not treated as a directly observed empirical fleet capacity
$FCost_v^1$	Relative scale (freezer > refrigerated)	Goentzel et al. (2023)	Structured modeling assumption	Freezer-equipped vehicles were assigned higher fixed costs than refrigerated vehicles to reflect the additional infrastructure and cold-chain requirements. This parameter is treated as a structured modeling assumption rather than an observed procurement cost
$FCost_v^2$	Proportionally lower than $FCost_v^1$	Structured assumption	Structured modeling assumption	Specified proportionally lower than $FCost_v^1$ to reflect the lower operational requirements of intra-provincial transportation
$Ecost_m$	Relative cost coefficient distinguishing refrigerated and freezer-equipped vehicle configurations	United Nations Children's Fund (UNICEF) (2025), World Health Organization (2024a, 2024b)	Price-data-supported structured scenario coefficient	Represents the relative cost difference between refrigerated and freezer-equipped transportation configurations. Because publicly available vehicle-specific procurement costs were unavailable for the case study, this coefficient was specified as a structured scenario parameter informed by UNICEF cold-chain equipment price data and WHO PQS equipment classifications. It is not intended to reproduce actual vehicle procurement costs but to represent the additional cost associated with stricter cold-chain requirements in scenario and sensitivity analyses

(***continued***)

Downloaded from www.emerald.com/jhlscm/article-pdf/doi/10.1108/JHLSCM-11-2025-0229/11895066/jhlscm-11-2025-0229en.pdf by University of Sheffield user on 29 October 2026

Table 4

Parameter	Value/range used in this study	Source	Source type	Calibration/justification
$Pallet_v$	Vaccine-type-specific number of doses per pallet or shipment unit	World Health Organization (2017) World Health Organization (2012) World Health Organization (2021a)	Packaging-based calculated scenario input	Represents the vaccine-type-specific number of doses associated with the shipment unit used in the model. The value is calculated from vaccine presentation, doses per vial, vials per carton, cartons per case and packaging configuration following WHO vaccine-volume guidance. For ultra-cold-chain vaccines, manufacturer thermal shippers are represented as shipment units within this parameter. Values should be updated whenever manufacturer-specific packaging specifications are available
$Cost_v$	Scenario-based magnitude differentiation across vaccine types	Literature-informed magnitude (Rastegar et al., 2021)	Literature-informed scenario assumption empirically reported	Structured within empirically reported procurement cost levels while allowing scenario-based differentiation
Ds_t	Truncated Poisson distribution	Zhao et al. (2021)	Modeling assumption	A truncated Poisson distribution is used to approximate disease spread over the planning horizon, following the Poisson-based epidemic modeling approach reported by Zhao et al. (2021)
Pop'^{j}_{zg}	Census-based population	Statistical left of Iran (2026)	Empirically observed	Population data are based on publicly available census statistics
α	Literature-aligned COVID mortality rate	Hasan et al. (2021) Ioannidis (2020) Meyerowitz-Katz and Merone (2020)	Literature-based	Aligned with published COVID-19 CFR/IFR evidence used to define a representative population-level mortality parameter
$VehType_{mv}$	Vehicle–vaccine compatibility	Objio et al. (2024), World Health Organization (2024a, 2024b)	Literature-based	Vehicle–vaccine compatibility is derived from vaccine-specific storage and transport temperature requirements. Vehicles providing freezer or refrigerated cold-chain conditions are assigned only to vaccines whose recommended temperature ranges can be maintained throughout transportation, consistent with CDC vaccine storage and handling guidance and WHO cold-chain equipment specifications
$Rate_v$	Small vaccine-type-specific spoilage/wastage coefficient, calibrated around closed-vial supply-chain wastage assumptions	World Health Organization (2025), World Health Organization (2021b)	WHO wastage-guided calibrated scenario input	represents vaccine losses occurring before administration due to spoilage, cold-chain disruption, expiry, breakage or other storage/transport-related losses. Because the model deducts spoilage from delivered vaccines before administration, this parameter is interpreted as a closed-vial/supply-chain wastage coefficient rather than open-vial session wastage. WHO guidance distinguishes closed-vial wastage from opened-vial wastage and treats closed-vial losses as supply-chain losses occurring across storage and distribution levels. In the absence of publicly available Iran-specific vaccine spoilage data, $Rate_v$ is treated as a WHO-guided calibrated scenario input, with values kept small and adjustable through scenario or sensitivity analysis

(***continued***)

Downloaded from www.emerald.com/jhlscm/article-pdf/doi/10.1108/JHLSCM-11-2025-0229/11895066/jhlscm-11-2025-0229en.pdf by University of Sheffield user on 29 October 2026

Table 4

Parameter	Value/range used in this study	Source	Source type	Calibration/justification
Dr_g^j	Age-specific prevalence consistent with COVID studies	Fadaki et al. (2022) Hasan et al. (2021)	Literature-calibrated scenario input	Calibrated using published age-specific COVID-19 epidemiological studies and represented through a time-dependent prevalence function
Distances	Approximate inter-provincial distances derived from geographic coordinates	Iran National Cartographic left (2026) Baktash (2012)	Geospatial data	Inter-provincial distances were approximated using publicly available geographic coordinate/map data from the Iran National Cartographic left. These distances are treated as empirically observed spatial inputs and are used to represent the geographic structure of the distribution network and calculate transportation costs
Behavioral adaptation thresholds (85%, 90%, 95%; 1%, 3%, 5%)	Piecewise-linear thresholds	This study; supported conceptually by (Bauch and Galvani, 2013) and (Roy et al., 2022)	Modeling assumption	Introduced as transparent modeling assumptions representing high, very high, and near-saturation vaccination uptake regimes. The associated step increases provide bounded and monotonic positive behavioral reinforcement rather than empirically estimated thresholds

Source(s): Authors' own work

This representation reflects widely observed pandemic averages while enabling the model to simulate realistic epidemic outcomes. Disease prevalence is incorporated through a time-dependent function embedded in the multiobjective optimization framework, allowing infection dynamics to evolve over the planning horizon rather than replicating specific historical outbreak trajectories. This design supports scenario-based analysis and avoids reliance on incomplete or rapidly changing epidemiological data sets.

3.6.3 Cold-chain, storage, vehicle-capacity and packaging data

Cold-chain and capacity-related parameters were treated as standards-guided calibrated scenario inputs rather than purely arbitrary assumptions. Exact operational capacities of national and provincial vaccine stores, refrigerated vehicles and freezer-compatible vehicles were not publicly available. Therefore, refrigerated storage capacity $\left(Cap_t^R\right)$ and freezer storage capacity (Cap_t^F) were calibrated using WHO/UNICEF vaccine storage-capacity guidance and standard walk-in cold-room/freezer-room configurations. Refrigerated storage was represented using standard walk-in cold-room sizes of 10, 30 or 40 m^3, while freezer storage was represented using 15–20 m^3 freezer-room capacity or a 15 m^3 freezer compartment in a combined cold/freezer-room configuration. These volume-based capacities were converted into dose capacity using vaccine-volume calculation procedures.

Vehicle-capacity parameters were treated similarly. The inter-provincial vehicle-capacity parameter (Cap_{jm}^{Vac}) was specified using representative small, medium and large vehicle-type capacity levels. These levels were calibrated using WHO-PQS refrigerated vehicle guidance, where net usable capacity is calculated as a proportion of gross vehicle cargo volume. The intra-provincial capacity parameter $(Cap_{jm}^{Vac'})$ was specified at a smaller scale to reflect local or last-mile delivery. It was calibrated using WHO/UNICEF guidance on vaccine carriers and cold boxes, which are commonly used for movement between vaccine stores and health facilities.

Vaccine–vehicle compatibility $(VehType_{mv})$ was defined according to vaccine-specific temperature requirements. Vaccine type V1 was assigned to freezer-compatible transport, while vaccine types V2 and V3 were assigned to refrigerated transport. The pallet parameter $(Pallet_v)$ was treated as a packaging-based calculated scenario input, depending on doses per vial, vials per carton, cartons per case and cases per pallet. For frozen or ultra-cold-chain vaccines, thermal shipper capacity can also be interpreted as a pallet-equivalent shipment unit. Finally, the vaccine spoilage parameter $(Rate_v)$ was interpreted as a closed-vial, preadministration supply-chain wastage coefficient, capturing losses due to cold-chain disruption, expiry, breakage or stock-management problems during storage and transport. In the absence of Iran-specific spoilage data, this parameter was specified as a small WHO-guided scenario value and retained for sensitivity analysis.

3.6.4 Transportation, routing and economic data.

Inter-provincial distances were approximated using geographic coordinates obtained from publicly accessible map data from the Iran National Cartographic Center. These distances were used to represent the spatial structure of the distribution network and to calculate transportation costs. The number of provinces and their administrative relationships correspond to Iran's actual territorial divisions.

Because detailed operational cost data were not publicly available, transportation cost parameters were calibrated within

Downloaded from www.emerald.com/jhlscm/article-pdf/doi/10.1108/JHLSCM-11-2025-0229/11895066/jhlscm-11-2025-0229en.pdf by University of Sheffield user on 29 October 2026

literature-documented numerical ranges reported in comparable vaccine supply chain optimization studies. Specifically, inter-provincial transportation cost (CPK^1) was calibrated in alignment with the magnitude reported by Goentzel *et al.* (2023), who report a representative vehicle operating cost of approximately 0.6 USD/km in a vaccine distribution network case study. Accordingly, CPK^1 was specified within the range of 0.5–0.8 US$/km, centered around 0.6 US$/km, to reflect uncertainty in longer-distance vaccine distribution costs. Intra-provincial transportation cost (CPK^2) was specified within the range of 0.3–0.5 US$/km, corresponding to approximately 60–70% of CPK^1, to reflect shorter routing distances, reduced fuel consumption, and lower logistical intensity within provinces.

Vaccine procurement cost ($Cost_v$) was treated as a literature-informed scenario parameter. Rastegar *et al.* (2021) report procurement-cost magnitudes for vaccine distribution modeling in an Iranian case context. In the present study, vaccine costs were structured within comparable literature-informed magnitudes while allowing scenario-based differentiation across vaccine types. This differentiation reflects the possibility that vaccine types may differ in procurement price, import requirements and cold-chain handling needs. These values are therefore not presented as observed procurement contracts, but as transparent scenario inputs aligned with prior vaccine distribution modeling studies.

Vehicle fixed-cost parameters ($FCost_v^1$ and $FCost_v^2$) were treated as structured modeling assumptions rather than observed procurement prices. Exact country-specific acquisition costs for refrigerated and freezer-compatible vehicles were not publicly available. Therefore, the model uses a relative fixed-cost structure in which larger vehicle types have higher fixed costs, freezer-compatible vehicles have higher fixed costs than refrigerated vehicles, and intra-provincial vehicle fixed costs are specified proportionally lower than inter-provincial vehicle fixed costs. The coefficient $Ecost_m$ was used to represent the relative cost difference between refrigerated and freezer-compatible configurations. This coefficient was specified as a price-data-supported structured scenario parameter, informed by the general cost variation observed across cold-chain equipment categories, but it does not claim to reproduce exact vehicle procurement prices.

Overall, the economic parameters were specified to remain consistent with the magnitude and structure used in comparable vaccine logistics and humanitarian supply-chain optimization studies, while avoiding unsupported claims of direct empirical observation. In pandemic logistics contexts, detailed operational cost data are often unavailable because of confidentiality constraints, emergency procurement practices and rapidly changing contracting conditions. For this reason, the numerical example is intended for structural and policy-oriented analysis rather than precise historical cost replication. By distinguishing empirically observed data, literature-calibrated estimates, standards-guided scenario inputs and structured modeling assumptions, the model maintains transparency, reproducibility and methodological comparability while enabling evaluation of tradeoffs among cost, mortality and equity objectives.

3.7 Data limitations and humanitarian context constraints

Detailed operational microlevel cost data are rarely publicly accessible during pandemic response due to emergency procurement procedures, rapidly evolving logistics configurations and institutional confidentiality constraints. Consequently, many humanitarian logistics optimization studies adopt structured scenario-based calibration approaches when exact cost accounting data are unavailable (e.g. Fadaki *et al.*, 2022; Goentzel *et al.*, 2023; Tavana *et al.*, 2026). Consistent with this practice, the present study integrates publicly available demographic, epidemiological and spatial data, while calibrating cost parameters within literature-supported magnitudes. This approach ensures structural realism without claiming direct operational auditing of real-world distribution expenditures. In particular, vaccine procurement prices during pandemic conditions are subject to contract-specific negotiations, international supply constraints and confidential purchasing agreements. Therefore, procurement costs in this study are modeled at representative magnitude levels rather than exact contractual values.

3.8 Software and execution

The model was implemented and solved using the General Algebraic Modeling System. The computational time required to solve the initial scenario (using the predefined vehicle types) was approximately 43 min. The main decision variable results for this scenario are summarized in Tables 5 and 6, corresponding to inter-provincial (x) and intra-provincial (y) vaccine shipments.

3.9 Initial scenario

The initial scenario represents a simplified but comprehensive case designed to demonstrate the model's operational structure and internal consistency. The network includes a single national distribution center (indexed as *J01*) supplying one hub province (*J02*) and six nonhub provinces (*J03–J08*) across a 24-week planning horizon. The detailed description of the initial scenario is presented in Appendix C.

3.10 Computational justification and model complexity

The baseline scenario, although simplified in network size, incorporates a multiperiod, multiproduct and multiechelon structure with binary routing and vehicle activation decisions. The resulting formulation includes binary variables for inter- and intra-provincial routing, binary variables for vehicle activation and sequencing, continuous variables for vaccine flows and administration and auxiliary variables for sub-tour elimination and behavioral adaptation. Even in the baseline configuration (one distribution center, one hub province and six nonhub provinces over 24 periods), the model contains several thousand decision variables and constraints. The inclusion of vehicle routing and sub-tour elimination constraints introduces combinatorial complexity characteristic of NP-hard routing and network design problems widely recognized in operations research literature (e.g. Lim *et al.*, 2022; Smalley *et al.*, 2015).

The number of routing variables grows approximately with the square of the number of nodes [$O(n^2)$] per period, while the multiperiod structure multiplies this complexity by the

Downloaded from www.emerald.com/jhlscm/article-pdf/doi/10.1108/JHLSCM-11-2025-0229/11895066/jhlscm-11-2025-0229en.pdf by University of Sheffield user on 29 October 2026

Table 5 Amount of vaccine type *v* transported from the Central distribution center to the hub province via air transport in each period *t* (illustrative example with One origin and One hub)

Vaccine type	T01	T02	T03	T04	T05	T06	T07	T08	T09	T10	T11	T12	T13	T14	T15	T16	T17	T18	T19	T20	T21	T22	T23	T24
V1	2,000	2,525	2,044	110	204	689	5,556	0	1,204	2,188	2,738	1,001	4,049	0	3221	6333	5919	1399	4781	1272	309	3678	306	3349
V2		691				2,197	2,001	804		2,001		1,001					2020		271					
V3		3,198			204	8,000	3,094	841	1,001	3,238	1,001	3,115		4,421		2440	566	106	47	33	6782	100	1000	3128
Total (V1+V2+V3)	2,000	6,414	2,044	110	408	10,886	10,651	1,645	2,205	7,427	3,739	5,117	4,049	4,421	3221	8773	8505	1505	5099	1305	7091	3778	1306	6477

Source(s): Authors' own work

Downloaded from www.emerald.com/jhlscm/article-pdf/doi/10.1108/JHLSCM-11-2025-0229/11895066/jhlscm-11-2025-0229en.pdf by University of Sheffield user on 29 October 2026

Table 6 Amount of vaccine type v transported from origin province (distribution center or hub) to destination provinces using vehicle type m in each period t (illustrative example)

Origin province	Vaccine type	Vehicle type	J03	J04	J05	J06	J07	J8
J01	V1	m08	22,893		13,598			9,919
J01	V1	m09		5,191				
J01	V1	m10				12,037	13,189	
J01	V2	m03	7,522					
J01	V2	m01		2,527	14,877			
J01	V2	m02					23,606	
J01	V2	m03				18,052		21,522
J01	V3	m01					28,535	
J01	V3	m02		45,787	29,695			
J01	V3	m03	24,463			28,695		36,162
J02	V1	m08				9,016	3,888	
J02	V1	m08		6,291	6,019			
J02	V2	m01		2	3,469		2	3,095
J02	V3	m01			3			
J02	V3	m01	9,606	6,293			3,094	

Source(s): Authors' own work

planning horizon. Vehicle activation and compatibility constraints further increase the solution space due to binary decision interactions. Consequently, extending the model to full national or multicountry networks would significantly increase computational requirements. However, this growth pattern is consistent with vehicle routing and humanitarian logistics optimization models reported in the literature.

The baseline scenario demonstrates that the integrated formulation is computationally solvable using exact methods for moderate network sizes. The proposed model is intended as a decision-support framework for scenario analysis and preparedness planning rather than a real-time operational tool. The baseline instance demonstrates computational feasibility for moderate network sizes while revealing structural insights relevant to policy design. It focuses on formulation and structural insights, providing a foundation for such scalable solution approaches in future research. This positioning clarifies that the primary contribution of the study lies in the development of an integrated modeling framework, while scalability to large-scale instances and the design of advanced solution approaches are identified as important directions for future research.

For large-scale national or multicountry applications, several strategies may support scalability: decomposition approaches, separating strategic allocation from operational routing; rolling-horizon planning, enabling sequential decision updates as new data become available; metaheuristic algorithms, such as genetic algorithms or large neighborhood search, to approximate solutions for large routing networks; and scenario reduction techniques, focusing on representative demand and behavioral patterns.

Importantly, pandemic decision-making often occurs under severe time pressure and data uncertainty. In such contexts, scenario-based planning tools can provide valuable guidance even when exact large-scale optimization is not feasible. The framework presented here supports exploration of policy alternatives and structural tradeoffs, enabling more informed preparedness and response planning.

Table 5 summarizes the total amount of vaccine type v sent from the distribution center (where $o = 1$) to the hub province (where $u = 1$) in each period t, via air transport. This example illustrates a simplified case with a single origin and a single hub.

The last row reports the total amount of vaccines (sum of V1, V2 and V3) sent to the hub province in each period. Table 5 presents the amount of vaccine type v sent from J01 (the central distribution center) and J02 (the hub province) to destination provinces J03 through J08 using vehicle type m during each period t. Both origin and destination provinces are indexed using j, but only J01 and J02 serve as origins in this example, while J03–J08 are recipient provinces. This table reflects a scenario with one distribution center and one hub province.

Each province in the model, including the hub, is subdivided into a set of intra-provincial regions denoted by z. The index $z = 0$ represents the provincial center where vaccines arrive, and $z \neq 0$ refers to interior regions that receive vaccines via local routes. In this illustrative example, each province is assumed to contain three interior regions ($z = 1, 2, 3$) in addition to the provincial center ($z = 0$). This structure activates all intra-provincial routing, vehicle-capacity and sub-tour elimination constraints, ensuring that the local distribution level is represented even though only one distribution center and one hub province are explicitly shown in Tables 5 and 6.

Analysis of the results indicates that Province J01 fully uses its fleet of three vehicles from both vehicle categories, freezer-equipped (F-type vehicles) and refrigerated (R-type vehicles), whereas Province J02 operates only one vehicle from each category.

4. Results

The proposed bi-objective MILP optimization model was implemented using context-informed demographic inputs and literature-calibrated epidemiological and logistical parameters within a scenario-based framework inspired by the COVID-19 vaccination context in Iran. The model successfully identified optimal shipment quantities, vehicle allocation patterns, and routing strategies across a 24-week planning horizon.

Key results are summarized below:

- *Efficient allocation of vaccine types*
  The model ensured timely and appropriate delivery of three vaccine types, one requiring freezing conditions (V1) and two requiring refrigeration (V2, V3). Shipments from the central distribution center ($o = 0$) to hub provinces ($u \in U$) were made via air transport, as detailed in Table 5. From there, inter-provincial and intra-provincial routing took place overland using temperature-compatible vehicles.
- *Cost and coverage optimization*
  The model illustrates the cost-mortality tradeoff while allocating vaccines across provinces and age groups under the modeled constraints. This tradeoff was achieved through the weighted fuzzy goal programming formulation. Table 3 presents the tradeoff values derived from the payoff matrix, illustrating the compromise obtained between the two objective functions. Within the proposed weighted fuzzy goal programming formulation,

Downloaded from www.emerald.com/jhlscm/article-pdf/doi/10.1108/JHLSCM-11-2025-0229/11895066/jhlscm-11-2025-0229en.pdf by University of Sheffield user on 29 October 2026

assigning greater importance to the mortality objective would lead the model to allocate available vaccines in a manner that further reduces mortality within the existing transportation, routing, cold-chain and capacity constraints, whereas assigning greater importance to the cost objective would result in solutions with lower total distribution cost. Therefore, the proposed formulation provides a compromise solution between minimizing the total distribution cost and minimizing mortality under the modeled constraints.

- *Vehicle allocation and utilization*
  The model determined the optimal number and type of vehicles (freezer-equipped vs. refrigerated) needed in each province. For example, Province J1 fully used three vehicles from both Type 1 (freezer) and Type 2 (refrigerated) classes, while Province J2 deployed only one vehicle of each type. This assignment respected the cold chain constraints and minimized fixed vehicle costs.
- *Temporal dynamics of distribution*
  As seen in Table 5, vaccine deliveries were dynamically adjusted over time. Early weeks prioritized hub provinces with large populations and high-risk demographics. The adaptive vaccination rate ensured that areas with faster public uptake received proportionally more doses in subsequent weeks, supporting behavioral alignment.
- *Mortality and coverage outcomes*
  The model indicates how prioritization of age group 3 (30–55), as specified in Constraint 35, influences projected deaths within the modeled structure.
- *Equity and cold chain integrity*
  The fairness constraints ensured each province received vaccines proportional to its at-risk population, while respecting the limited supply. All vaccine shipments were assigned to vehicles compatible with the required storage conditions, ensuring cold chain integrity was preserved throughout the network.

These results illustrate how the proposed model can support structured decision-making in pandemic vaccine logistics under the modeled assumptions. They also serve as the baseline scenario for further sensitivity analyses, where variations in vehicle capacity and disease spread rate are evaluated.

4.1 Baseline policies and benchmarking scope

To facilitate interpretation, a proportional allocation policy is defined as a commonly used benchmark in public health logistics: in each period, available doses are distributed across provinces in proportion to their population shares. In the present study, the numerical example represents the baseline scenario under the proposed optimization framework, and the corresponding results are presented below. These baseline results include the total distribution cost, mortality outcomes and allocation patterns across provinces under the integrated optimization framework. While the proportional allocation policy is explicitly defined, a full quantitative comparison between this benchmark and the proposed model is beyond the scope of the present study, as this would require implementing and solving the alternative policy under the same network and operational constraints.

This is identified as a direction for future research. From a structural perspective, however, proportional allocation does not explicitly internalize routing feasibility, heterogeneous vehicle capacities, cold-chain compatibility constraints or vehicle activation costs, nor does it directly incorporate mortality minimization or age-based prioritization within its allocation logic. As a result, while proportional allocation ensures population-based fairness in a static sense, it does not guarantee feasibility or Pareto-efficient tradeoffs under binding capacity and logistics constraints. The proposed bi-objective optimization framework, by contrast, simultaneously integrates allocation, routing, vehicle activation, cold-chain compatibility and mortality considerations within a unified mathematical structure. The present study therefore emphasizes structural comparison and tradeoff analysis.

4.2 Preference-weight analysis of the cost–mortality tradeoff

Because the proposed model is bi-objective, the relative importance assigned to cost minimization and mortality reduction can influence the resulting allocation and routing decisions. To make this tradeoff more explicit, Table 7 presents a preference-weight scenario analysis in which the cost weight w_1 and mortality-reduction weight w_2 are varied from a cost-dominant setting to a mortality-dominant setting. The balanced case, where $w1 = 0.50$ and $w2 = 0.50$, corresponds to the baseline solution reported in the numerical results.

The results show the expected tradeoff between logistics cost and mortality reduction. When the cost weight is increased, the model favors lower-cost distribution patterns, resulting in lower total distribution cost but a higher projected number of fatalities. This reflects a more conservative use of vehicle capacity and routing options. In contrast, when the mortality-reduction weight is increased, the model accepts higher distribution cost to support earlier and broader vaccine delivery to high-risk or high-prevalence population groups.

The balanced baseline solution produces a compromise between these two extremes. Compared with the cost-dominant scenario, it requires higher logistics expenditure but avoids additional fatalities. Compared with the mortality-dominant scenario, it does not achieve the lowest possible fatality level, but it avoids the highest logistics cost. This analysis therefore demonstrates how the proposed model can support policy discussion by showing how much additional distribution cost may be required to achieve further reductions in mortality.

5. Sensitivity analysis

In the present research, two important sensitivity analyses were undertaken. This sensitivity analysis is designed not only to evaluate model responsiveness but also to examine the robustness of outcomes under parameter uncertainty, particularly in contexts where certain epidemiological or operational inputs may not be precisely observable.

5.1 Vehicle capacity

The first sensitivity analysis focused on the inter-provincial vehicle capacity, examining scenarios where the capacity was

Downloaded from www.emerald.com/jhlscm/article-pdf/doi/10.1108/JHLSCM-11-2025-0229/11895066/jhlscm-11-2025-0229en.pdf by University of Sheffield user on 29 October 2026

Downloaded from www.emerald.com/jhlscm/article-pdf/doi/10.1108/JHLSCM-11-2025-0229/11895066/jhlscm-11-2025-0229en.pdf by University of Sheffield user on 29 October 2026

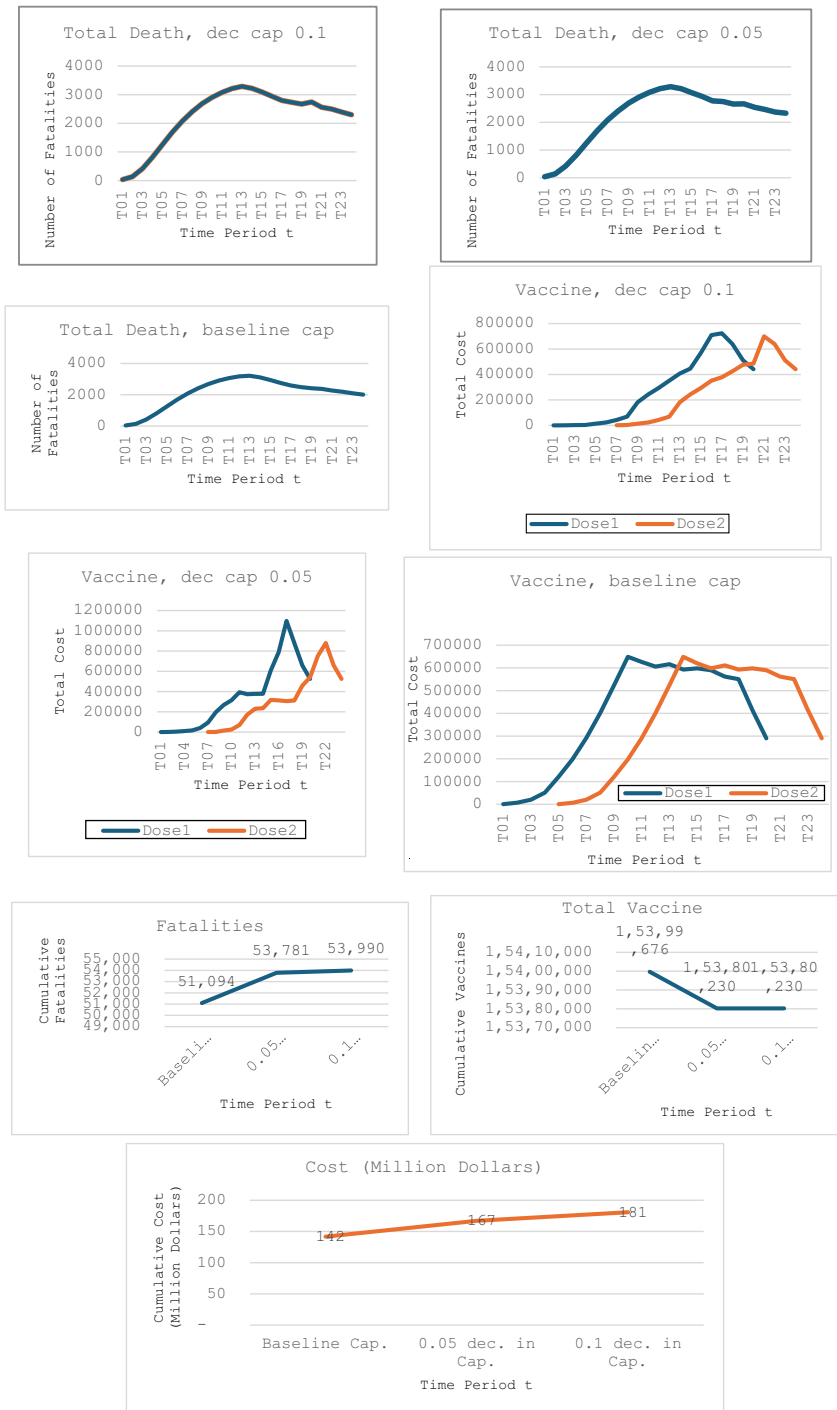
Table 7 Preference-weight analysis of the cost–mortality tradeoff

Scenario	Cost weight w_1	Mortality weight w_2	Total distribution cost, million USD	Change in cost from baseline (%)	Total fatalities	Change in fatalities from baseline (%)	Total vaccines administered	Allocation and routing interpretation
S1: Cost-dominant	0.90	0.10	134.60	−5.00	53,649	+5.00	15,168,681	Stronger preference for cheaper routes and lower vehicle activation; later or more conservative delivery to some lower-priority regions
S2: Cost-sensitive	0.70	0.30	138.50	−2.25	52,116	+2.00	15,322,678	Moderate cost saving while still maintaining most baseline vaccination coverage
S3: Balanced baseline	0.50	0.50	141.69	0.00	51,094	0.00	15,399,676	Balanced compromise between cost minimization and mortality reduction
S4: Mortality-sensitive	0.30	0.70	150.19	+6.00	50,072	−2.00	15,476,674	Earlier allocation to high-risk/high-prevalence groups; additional or less cost-efficient routes may be activated
S5: Mortality-dominant	0.10	0.90	159.92	+12.87	49,561	−3.00	15,553,673	Strongest mortality-reduction preference; more aggressive early delivery and higher logistical effort

Source(s): Authors' own work

reduced by 5% and 10% compared to the baseline. Figure 3 presents the cumulative number of fatalities, the total number of vaccines administered, and the total distribution cost over time, across the three capacity scenarios (baseline, 5% reduction and 10% reduction). A 10% decrease in vehicle capacity leads to a 5.67% increase in fatalities, a 0.13% decrease in the total number of vaccines administered, and a 27.46% increase in costs compared to the baseline scenario. A 5% decrease in vehicle capacity results in a 5.27% increase in fatalities, a 0.13% decrease in the number of vaccines administered, and an 18.00% increase in costs compared to the baseline scenario.

Figure 3 Sensitivity analysis of vehicle capacity



Source: Authors' own work

Downloaded from www.emerald.com/jhlscm/article-pdf/doi/10.1108/JHLSCM-11-2025-0229/11895066/jhlscm-11-2025-0229en.pdf by University of Sheffield user on 29 October 2026

These results suggest that while the model effectively maintains vaccination coverage under reduced capacity by activating additional or less efficient transportation resources, this strategy comes at the expense of substantially higher costs. The model prioritizes minimizing fatalities and maintaining vaccination coverage, especially in high-risk populations and compensates for reduced capacity by using costlier vehicle types and longer routes, a tradeoff that leads to disproportionately higher costs despite relatively stable vaccine administration. This result provides important policy implications, as it shows decision-makers that reducing vehicle availability is a counterproductive strategy as it will in turn increase costs more than proportionally.

5.2 Disease spread rate

The second sensitivity analysis was conducted to assess the system's response to variations in the disease spread coefficient, which typically differs across epidemics. This analysis examines scenarios involving a 1% decrease, a 1% increase and a 2% increase relative to the baseline. These percentage variations were selected to represent small but meaningful deviations around the baseline disease spread rate, allowing assessment of model sensitivity and robustness under modest epidemiological uncertainty without introducing extreme or unrealistic scenarios. Figure 4 presents the cumulative number of fatalities, the total number of vaccines administered, and the combined overview of both metrics over time across the four disease spread scenarios (baseline, 1% decrease, 1% increase and 2% increase).

A 1% decrease in the disease spread coefficient leads to a 0.41% reduction in fatalities and no significant change in the number of vaccines administered compared to the baseline scenario. A 1% increase in the disease spread coefficient results in a 2.86% increase in fatalities and a 4.38% increase in the number of vaccines administered. These results show that as the disease spreads more rapidly, the system responds by accelerating vaccination efforts, but this also leads to a measurable rise in mortality, highlighting the critical importance of early intervention in controlling epidemic dynamics.

The sensitivity analysis confirms that the proposed model exhibits a measurable response to changes in the disease spread coefficient. These figures indicate that even slight variations in this parameter can influence both mortality and vaccine distribution volumes, which demonstrates the sensitivity of the model to epidemiological dynamics. While the model compensates for higher disease transmission by increasing vaccine allocation, the rise in fatalities highlights the limits of logistical responsiveness under more aggressive outbreak conditions.

6. Conclusion

This study proposes a comprehensive and adaptable bi-objective, multiproduct, multiperiod MILP model that addresses the urgent and complex challenge of vaccine allocation and distribution during pandemics. By combining cost minimization and mortality reduction objectives, the model contributes to the literature on operations research and public health logistics. Its novelty lies in the integration of inter- and intra-provincial distribution networks, adaptive vaccination rates based on public acceptance trends, cold chain compatibility between vaccine types and vehicle types, and the incorporation of vehicle activation and sequencing logic, components often overlooked in prior models. From a theoretical standpoint, this research extends existing vaccine logistics modeling by unifying multiple operational layers within a single decision-support framework. It contributes to the field by introducing a dynamic vaccination rate function informed by behavioral trends, thus bridging epidemiological modeling with optimization. The use of a piecewise linear trust-based vaccination function, along with detailed vehicle routing constraints, demonstrates how mathematical programming can more realistically reflect public health complexities. Furthermore, the application of Lin's weighted max–min fuzzy goal programming approach offers a refined method for balancing conflicting objectives on different scales.

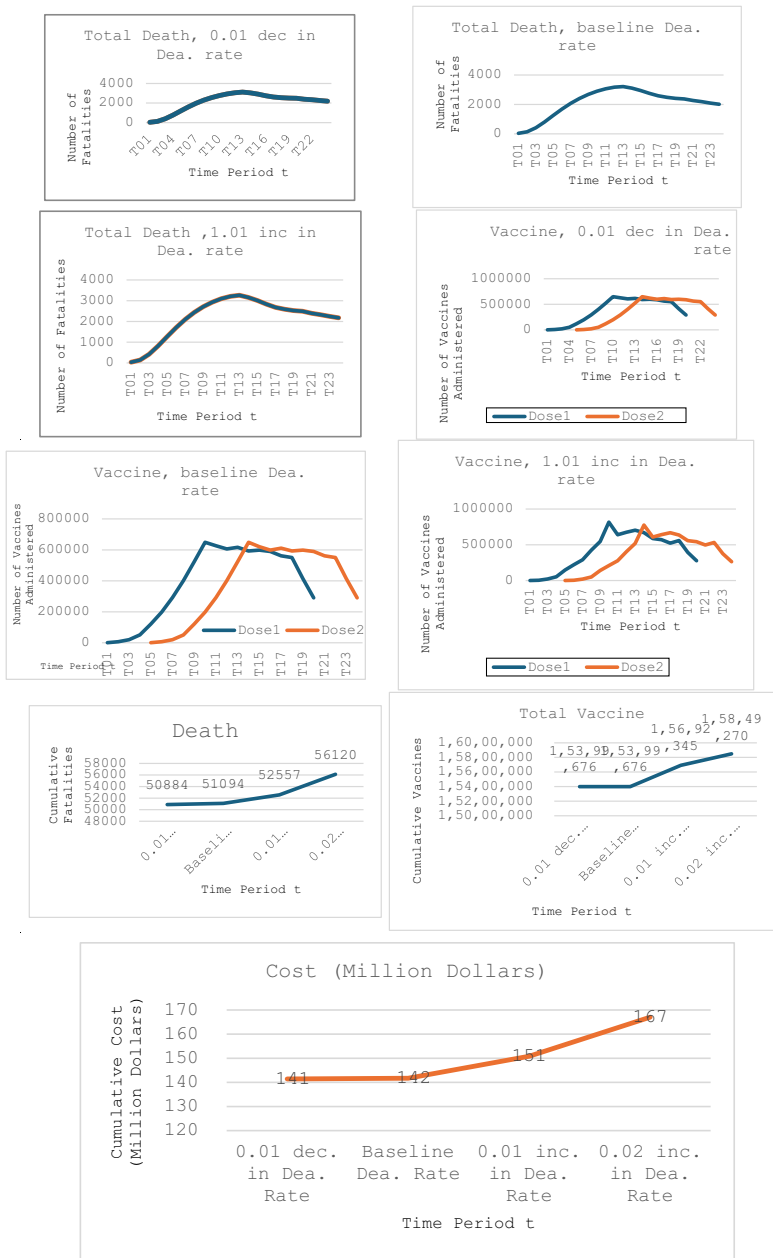
In terms of practical implications, the model provides a strategic decision-support framework that can inform policymakers, health authorities and logistics planners in pandemic preparedness and response. Its scenario-based illustration inspired by the COVID-19 vaccination context in Iran highlights its potential relevance in settings where infrastructure and resource constraints coexist with urgent public health demands. Ministries of Health, for instance, can use the model as a scenario-analysis framework to explore cost-aware and equity-oriented vaccine distribution strategies that respond to changing public uptake and regional risk profiles. Rather than supporting real-time operational decisions, the proposed framework is intended for advance planning and scenario-based analysis, enabling policymakers to prepare and evaluate response strategies before time-critical implementation is required. For example, the sensitivity analysis results showing that reduced vehicle capacity leads to substantial increases in distribution costs is an important insight for policy makers, urging them to plan for enough vehicle capacity when designing their distribution plans. Moreover, the built-in flexibility allows adaptation to different vaccine types, delivery vehicles and regional contexts, making it potentially useful for national and international pandemic response planning.

The ability to generate structured comparisons of cost-mortality tradeoffs under varying epidemiological and capacity conditions supports evidence-based policy deliberations prior to crisis escalation. By translating complex epidemiological and logistical interactions into quantifiable policy tradeoffs, the model creates a structured interface between theoretical optimization and practical pandemic planning.

Although the proposed model provides a comprehensive vaccine allocation and distribution framework, its practical implementation requires different types of data with varying levels of availability during a pandemic. Some inputs, such as population size, administrative boundaries, age-group structure and approximate geographic distances, are usually available from census data and public geospatial sources. Other inputs, such as real-time disease prevalence, vaccine acceptance, cold-chain capacity, vehicle availability, spoilage rates and procurement/transport costs, may be more difficult to obtain during a pandemic because they are updated frequently, fragmented across agencies, commercially confidential or

Downloaded from www.emerald.com/jhlscm/article-pdf/doi/10.1108/JHLSCM-11-2025-0229/11895066/jhlscm-11-2025-0229en.pdf by University of Sheffield user on 29 October 2026

Figure 4 Sensitivity analysis on the disease spread rate



Source: Authors' own work

affected by emergency procurement conditions. Therefore, the model is best interpreted as a decision-support framework that can operate at different levels of detail depending on data availability.

Table 8 summarizes the main data requirements for implementing the model, their likely availability during a pandemic, and possible simplifications for time-sensitive decision-making. In a full preparedness-planning setting, the model can use detailed province-level, vehicle-level, vaccine-specific and period-specific data. In an emergency setting, however, a simplified version can be implemented by aggregating smaller regions into larger demand zones, reducing the number of vehicle and vaccine types, using pre-defined feasible routes, replacing detailed behavioral adaptation with low/medium/high uptake scenarios, and updating the model through a rolling-horizon approach as more reliable information becomes available.

This tiered implementation logic allows the model to remain useful even when detailed data are incomplete. The full version supports preparedness planning and post-hoc policy evaluation, while the simplified version can support rapid allocation decisions during the early stages of a pandemic. In this way, the proposed framework is not dependent on perfect real-time data; rather, it can be adapted to different decision

Downloaded from www.emerald.com/jhlscm/article-pdf/doi/10.1108/JHLSCM-11-2025-0229/11895066/jhlscm-11-2025-0229en.pdf by University of Sheffield user on 29 October 2026

Table 8 Main data requirements for implementing the proposed model, their likely availability during a pandemic and possible simplifications for rapid decision-making

Main data category	Likely availability during a pandemic	Possible simplification for rapid decision-making
Population size	Usually available from census statistics	No simplification generally required
Administrative boundaries	Usually available from public administrative records	No simplification generally required
Age-group structure	Usually available, although detailed local distributions may be limited	Use representative demographic proportions
Geographic distances	Usually available from public geospatial sources	Use approximate distance matrices where necessary
Disease prevalence	Frequently updated and subject to reporting delays	Use low-, medium- or high-transmission scenarios
Vaccine availability	May vary because of supply uncertainty	Aggregate vaccine availability by planning period
Vaccine acceptance (behavioral adaptation)	Difficult to estimate reliably in real time	Replace dynamic behavioral adaptation with scenario-based uptake assumptions
Cold-chain capacity	May be incomplete or fragmented across agencies	Use representative storage-capacity categories
Vehicle availability	May change during emergency operations	Reduce the number of vehicle types
Transportation and procurement costs	Often commercially confidential or rapidly changing	Use literature-calibrated representative values
Transportation network	Operational conditions may change	Use predefined feasible routes and aggregate smaller regions into larger demand zones; update the model using a rolling-horizon approach as new information becomes available

Source(s): Authors' own work

contexts by trading off modeling detail against speed and data availability.

In sum, this study not only offers a robust mathematical formulation but also a decision-support modeling framework that can inform data-driven decisions in future pandemics and public health emergencies. As vaccine equity and supply chain resilience become global imperatives, this model provides a foundation for analyzing tradeoffs in life-saving intervention planning.

From a comparative perspective, the proposed framework addresses several limitations observed in existing studies. While existing models contribute significantly to specific domains such as cold chain integrity, equitable allocation and multiechelon network design, most address only isolated facets of the broader operational challenge. In particular, inter- and intra-provincial distribution decisions, equity considerations and vehicle-level operational constraints are often modeled separately rather than within a unified optimization framework. As a result, the coordination between logistical feasibility and equitable access remains limited in much of the existing literature. Unlike many existing models that treat inter-provincial and intra-provincial distribution as separate processes, the proposed framework integrates both levels into a unified optimization structure, thereby ensuring coordination and improving overall logistical efficiency. A distinctive feature of this model is the explicit inclusion of fleet management decisions, recognizing their critical role in sustaining uninterrupted vaccine delivery operations, an aspect that is not always explicitly modeled in prior studies. In this study, fleet management decisions refer to the activation, assignment and sequencing of vehicle types across inter- and intra-provincial distribution stages, subject to capacity and vaccine-vehicle compatibility constraints. Unlike studies that consider fleet characteristics as fixed inputs, these decisions are endogenously determined within this optimization model. Furthermore, the model introduces a piecewise linear vaccination rate that dynamically adjusts based on previous public uptake, capturing fluctuations in behavioral response and enabling adaptive allocation strategies that reflect evolving public trust and demand. The model also supports the distribution of multiple vaccine types with differing storage requirements, ensuring that the compatibility between vaccine characteristics and transportation infrastructure, such as refrigerated or freezer-equipped vehicles, is rigorously maintained throughout the supply chain. Taken together, these features contribute to a comprehensive decision-support modeling framework that facilitates the analysis of key tradeoffs relevant to policymakers and public health logistics planners under pandemic conditions.

While this study provides a comprehensive framework for pandemic vaccine distribution, further research could: Integrate real-time demand forecasting for more adaptive distribution strategies; Extend the model to international vaccine logistics, addressing cross-border supply chain disruptions; Enhance equity-focused allocation frameworks, ensuring fair vaccine access across diverse demographic and socioeconomic groups.

Accordingly, the proposed framework can also serve as a methodological basis for future studies that incorporate more advanced behavioral adaptation mechanisms, integrate real-time demand forecasting and develop scalable solution approaches for larger pandemic vaccine distribution networks.

Despite the model's comprehensiveness, several limitations should be acknowledged. First, the problem is formulated as a single-level optimization model, whereas a bi-level structure may better reflect real-world policymaking, where government authorities prioritize public health outcomes over operational costs. Second, although air transportation costs are included in

Downloaded from www.emerald.com/jhlscm/article-pdf/doi/10.1108/JHLSCM-11-2025-0229/11895066/jhlscm-11-2025-0229en.pdf by University of Sheffield user on 29 October 2026

the objective function, the model assumes that shipments from the central distribution center to hub provinces are always performed by air. Consequently, the model does not optimize transportation-mode selection between air and ground alternatives for these shipments. Third, the behavioral adaptation component, modeled via a piecewise-linear vaccination rate, does not explicitly incorporate cultural, religious or region-specific trust factors, which may significantly affect vaccine uptake. In addition, the use of straight-line geographic distances between provinces, rather than road-based travel distances, may oversimplify inter-provincial routing. The model also assumes a uniform internal structure for all provinces and does not include subregional stratification, which may limit its scalability. Finally, while the model can be solved optimally for the current case study, larger problem instances may benefit from the development of tailored solution approaches, such as metaheuristic methods, to enhance computational tractability.

Accordingly, the numerical analysis is not intended to demonstrate large-scale performance, but rather to provide controlled and policy-relevant insights into the structural behavior of the proposed framework. A quantitative benchmark comparison against proportional allocation and other heuristics is not included in the current version due to the need for additional computational experiments, and is another important direction for future research.

References

AlJamaan, F., Temsah, M.H., Alhasan, K., Alenezi, S., Alhaboob, A., Alrabiaah, A., Batais, M., Alshahrani, F., Assiri, R.A., Bafaqih, H. and Alaraj, A. (2022), "SARS-CoV-2 variants and the global pandemic challenged by vaccine uptake during the emergence of the Delta variant: a national survey seeking vaccine", *Journal of Infection and Public Health*, Vol. 15 No. 7, pp. 773-780.

Andrews, N., Stowe, J., Kirsebom, F., Toffa, S., Rickeard, T., Gallagher, E., Gower, C., Kall, M., Groves, N., O'Connell, A.M. and Simons, D. (2022), "Covid-19 vaccine effectiveness against the omicron (B. 1.1. 529) variant", *New England Journal of Medicine*, Vol. 386 No. 16, pp. 1532-1546, doi: 10.1056/NEJMOA2119451.

Baktash, P. (2012), *National Report of Geomatics in Islamic Republic Of Iran*, United Nations Economic and Social Council, Bangkok.

Balcik, B., Yucesoy, E., Akca, B., Karakaya, S., Gevsek, A.A., Baharmand, H. and Sgarbossa, F. (2022), "A mathematical model for equitable in-country COVID-19 vaccine allocation", *International Journal of Production Research*, Vol. 60 No. 24, pp. 7502-7526.

Bauch, C. and Galvani, A. (2013), "Social and biological contagions", *American Association for the Advancement of Science*, Vol. 342 No. 6154, pp. 47-49.

Bellman, R.E. and Zadeh, L.A. (1970), "Decision-making in a fuzzy environment", *Management Science*, Vol. 17 No. 4, pp. B-141-B-164, doi: 10.1287/MNSC.17.4.B141.

Charnes, A., Cooper, W.W. and Ferguson, R.O. (1955), "Optimal estimation of executive compensation by linear programming", *Management Science*, Vol. 1 No. 2, pp. 138-151, doi: 10.1287/MNSC.1.2.138.

Chen, S.I., Norman, B.A., Rajgopal, J., Assi, T.M., Lee, B.Y. and Brown, S.T. (2014), "A planning model for the WHO-EPI vaccine distribution network in developing countries", *IIE Transactions (Transactions)*, Vol. 46 No. 8, pp. 853-865.

Cohn, B.A., Cirillo, P.M., Murphy, C.C., Krigbaum, N.Y. and Wallace, A.W. (2022), "SARS-CoV-2 vaccine protection and deaths among US veterans during 2021", *Science*, Vol. 375 No. 6578, pp. 331-336, doi: 10.1126/SCIENCE.ABM0620.

Dashraath, P., Wong, J.L.J., Lim, M.X.K., Lim, L.M., Li, S., Biswas, A. and Choolani, M. *et al.* (2020), "Coronavirus disease 2019 (COVID-19) pandemic and pregnancy", *American Journal of Obstetrics and Gynecology*, Vol. 222 No. 6, pp. 521-531.

de Figueiredo, A. and Larson, H.J. (2021), "Exploratory study of the global intent to accept COVID-19 vaccinations", *Communications Medicine*, Vol. 1 No. 1.

Delivorias, A. and Scholz, N. (2020), "Economic impact of epidemics and pandemics", European Parliamentary Research Service.

Enayati, S. and Özaltın, O. (2020), "Optimal influenza vaccine distribution with equity", *European Journal of Operational Research*, Vol. 283 No. 2, pp. 714-725.

Fadaki, M., Abareshi, A., Far, S.M. and Lee, P.T.W. (2022), "Multi-period vaccine allocation model in a pandemic: a case study of COVID-19 in Australia", *Transportation Research Part E: Logistics and Transportation Review*, Vol. 161, p. 102689.

Georgiadis, G.P. and Georgiadis, M.C. (2021), "Optimal planning of the COVID-19 vaccine supply chain", *Vaccine*, Vol. 39 No. 37, pp. 5302-5312.

Goentzel, J., Russell, T., Carretti, H.R. and Hashimoto, Y. (2023), "Vaccine network design to maximize immunization coverage", *Journal of Humanitarian Logistics and Supply Chain Management*, Vol. 13 No. 2, pp. 140-156.

Goodarzian, F., Ghasemi, P., Gunasekaren, A., Taleizadeh, A. A. and Abraham, A. (2022), "A sustainable-resilience healthcare network for handling COVID-19 pandemic", *Annals of Operations Research*, Vol. 312 No. 2, pp. 761-825.

Habibi, F., Abbasi, A. and Chakrabortty, R.K. (2023), "Designing an efficient vaccine supply chain network using a two-phase optimization approach: a case study of COVID-19 vaccine", *International Journal of Systems Science: Operations & Logistics*, Vol. 10 No. 1, p. 2121623.

Hasan, M.N., Haider, N., Stigler, F.L., Khan, R.A., Mccoy, D., Zumla, A., Kock, R.A. and Uddin, M.J. (2021), "The global case-fatality rate of COVID-19 has been declining since May 2020", *The American Journal of Tropical Medicine and Hygiene*, Vol. 104 No. 6, pp. 2176-2184.

Hegde, S., Mahmassani, H. and Smilowitz, K. (2023), "A two-regime analysis of the COVID-19 vaccine distribution process", *Journal of Humanitarian Logistics and Supply Chain Management*, Vol. 13 No. 2, pp. 111-124.

Ho, H.-P. (2019), "The supplier selection problem of a manufacturing company using the weighted multi-choice goal programming and MINMAX multi-choice goal programming", *Applied Mathematical Modelling*, Vol. 75, pp. 819-836.

Ioannidis, J. (2020), "Infection fatality rate of COVID-19 inferred from seroprevalence data", *Bulletin of the World Health Organization*, Vol. 99 No. 1, p. 265892.

Downloaded from www.emerald.com/jhlscm/article-pdf/doi/10.1108/JHLSCM-11-2025-0229/11895066/jhlscm-11-2025-0229en.pdf by University of Sheffield user on 29 October 2026

Ioannidis, J.P. (2021), "Reconciling estimates of global spread and infection fatality rates of COVID-19: an overview of systematic evaluations", *European Journal of Clinical Investigation*, Vol. 51 No. 5, p. 13554.

Iran National Cartographic Center (2026), "Iran national cartographic center", available at: www.ncc.gov.ir (accessed 20 September 2026).

Isermann, H. and Steuer, R.E. (1988), "Computational experience concerning payoff tables and minimum criterion values over the efficient set", *European Journal of Operational Research*, Vol. 33 No. 1, pp. 91-97.

Kamran, M., Kia, R., Goodarzian, F. and Ghasemi, P. (2023), "A new vaccine supply chain network under COVID-19 conditions considering system dynamic: artificial intelligence algorithms", *Socio-Economic Planning Sciences*, Vol. 85, p. 101378.

Kar, B. and Jenamani, M. (2025), "Optimizing a multimodal hub and spoke network for vaccine distribution using regional vulnerability index during healthcare emergencies", *Journal of Humanitarian Logistics and Supply Chain Management*, Vol. 15 No. 4, pp. 366-390.

Khodaee, V., Kayvanfar, V. and Haji, A. (2022), "A humanitarian cold supply chain distribution model with equity consideration: the case of COVID-19 vaccine distribution in the European Union", *Decision Analytics Journal*, Vol. 4, p. 100126.

Kochakkashani, F., Kayvanfar, V. and Haji, A. (2023), "Supply chain planning of vaccine and pharmaceutical clusters under uncertainty: the case of COVID-19", *Socio-Economic Planning Sciences*, Vol. 87, p. 101602.

Lazarus, J.V., Ratzan, S.C., Palayew, A., Gostin, L.O., Larson, H.J., Rabin, K., Kimball, S. and El-Mohandes, A. (2021), "A global survey of potential acceptance of a COVID-19 vaccine", *Nature Medicine*, Vol. 27 No. 2, pp. 225-228.

Lim, J., Norman, B.A. and Rajgopal, J. (2022), "Redesign of vaccine distribution networks", *International Transactions in Operational Research*, Vol. 29 No. 1, pp. 200-225.

Lin, C.-C. (2004), "A weighted max–min model for fuzzy goal programming", *Fuzzy Sets and Systems*, Vol. 142 No. 3, pp. 407-420.

Meyerowitz-Katz, G. and Merone, L. (2020), "A systematic review and meta-analysis of published research data on COVID-19 infection fatality rates", *International Journal of Infectious Diseases*, Vol. 101, pp. 138-148.

Moadab, A., Kordi, G., Paydar, M. and Divsalar, A. (2023), "Designing a sustainable-resilient-responsive supply chain network considering uncertainty in the COVID-19 era", *Expert Systems with Applications*, Vol. 227, p. 120334.

Objio, T., Morelli, V. and Trimble, S. (2024), "Vaccine storage and handling", in *Epidemiology and Prevention of Vaccine-Preventable Diseases (The Pink Book)*, Centers for Disease Control and Prevention (CDC), Atlanta, GA.

Qasem, A.G., Shamsan, A. and Aqlan, F. (2020), " "Optimal cholera vaccine allocation policies in developing countries: a case study", *Proceedings of the 5th NA International Conference on Industrial Engineering and Operations Management, MI.*

Rastegar, M., Madjid, T., Afshin, M. and Hassan, M. (2021), "An inventory-location optimization model for equitable influenza vaccine distribution in developing countries during the COVID-19 pandemic", *Vaccine*, Vol. 39 No. 3, pp. 495-504.

Rémy, V., York, Z. and Ulrike, H. (2015), "Vaccination: the cornerstone of an efficient healthcare system", *Market Access & Health Policy*, Vol. 3, pp. 1-6, doi: 10.3402/jmahp.v3.27041.

Ribeiro, D.J.B. (2016), "Design and planning of vaccine supply chains", Master's thesis, Instituto Superior Técnico, University of Lisbon.

Roy, D.N., Hossen, M.M., Ferdiousi, N. and Azam, M.S. (2022), "Potential factors influencing COVID-19 vaccine acceptance and hesitancy among Bangladeshi people: a cross-sectional study", *VirusDisease*, Vol. 33 No. 3, pp. 251-260, doi: 10.1007/s13337-022-00775-x.

Sallam, M., Al-Sanafi, M. and Sallam, M. (2022), "A global map of COVID-19 vaccine acceptance rates per country: an updated concise narrative review", *Journal of Multidisciplinary Healthcare*, Vol. 15, pp. 21-45.

Sarigol, I., Ozdemir, R. and Bayraktar, E. (2023), "Covid 19 vaccine order allocation: an optimization model with substitution", *Journal of Humanitarian Logistics and Supply Chain Management*, Vol. 13 No. 2, pp. 125-139.

Shahparvari, S., Hassanizadeh, B., Mohammadi, A., Kiani, B., Lau, K.H., Chhetri, P. and Abbasi, B. (2022), "A decision support system for prioritised COVID-19 two-dosage vaccination allocation and distribution", *Transportation Research Part E: Logistics and Transportation Review*, Vol. 159, p. 102598.

Shiri, M., Fattahi, P. and Sogandi, F. (2024), "Two-stage approach for COVID-19 vaccine supply chain network under uncertainty using the machine learning algorithms: a case study", *Engineering Applications of Artificial Intelligence*, Vol. 135, p. 108837.

Smalley, H.K., Keskinocak, P., Swann, J. and Hinman, A. (2015), "Optimized oral cholera vaccine distribution strategies to minimize disease incidence: a mixed integer programming model and analysis of a Bangladesh", *Vaccine*, Vol. 33 No. 46, pp. 6218-6223.

Solís Arce, J.S., Warren, S.S., Meriggi, N.F., Scacco, A., McMurry, N., Voors, M., Syunyaev, G., Malik, A.A., Aboutajdine, S., Adeojo, O. and Anigo, D. (2021), "COVID-19 vaccine acceptance and hesitancy in low-and middle-income countries", *Nature Medicine*, Vol. 27 No. 8, pp. 1385-1394.

Statistical Center of Iran (2026), available at: https://amar.org.ir/en (accessed 16 October 2025).

Sun, X., Andoh, E. and Yu, H. (2021), "A simulation-based analysis for effective distribution of COVID-19 vaccines: a case study in Norway", *Transportation Research Interdisciplinary Perspectives*, Vol. 11, p. 100453.

Taghipour, A., Sohrabi, A., Ghaedi, M. and Khazaei, M. (2023), "A robust vaccine supply chain model in pandemics: case of Covid-19 in Iran", *Computers & Industrial Engineering*, Vol. 183, p. 109465.

Tavana, M., Govindan, K., Nasr, A.K., Heidary, M.S. and Mina, H. (2026), "A mathematical programming approach for equitable COVID-19 vaccine distribution in developing countries", *Annals of Operations Research*, Vol. 360 No. 1, pp. 1-34.

Downloaded from www.emerald.com/jhlscm/article-pdf/doi/10.1108/JHLSCM-11-2025-0229/11895066/jhlscm-11-2025-0229en.pdf by University of Sheffield user on 29 October 2026

Thul, L. and Powell, W. (2023), "Stochastic optimization for vaccine and testing kit allocation for the COVID-19 pandemic", *European Journal of Operational Research*, Vol. 304 No. 1, pp. 325-338.

UNICEF Supply Division (2020), Walk-in cold rooms and freezer rooms supply division cold chain support package procurement guidelines procurement guidelines, UNICEF Supply Division, Copenhagen.

UNICEF Supply Division (2021), Procurement Guidelines: Vaccine Carriers and Cold Boxes, UNICEF Supply Division, Copenhagen, Denmark.

United Nations Children's Fund (UNICEF) (2024), "UNICEF supports the ministry of health and medical education by purchasing 19 walk-in cold rooms to preserve vaccine potency for children", available at: https://unicef.org/iran/en/press-releases/unicef-supports-ministry-health-and-medical-education-purchasing-19-walk-cold-rooms (accessed 20 September 2026).

United Nations Children's Fund (UNICEF) (2025), Solar-Powered Refrigeration Systems Price Data, UNICEF Supply Division, Copenhagen, Denmark.

Valizadeh, J., Boloukifar, S., Soltani, S., Hookerd, E., Fouladi, F., Rushchtc, A., Du, B. and Shen, J. (2023), "Designing an optimization model for the vaccine supply chain during the COVID-19 pandemic", *Expert Systems with Applications*, Vol. 214, p. 119009.

World Health Organization (2012), *User Guide for the WHO Vaccine Volume Calculator*, World Health Organization, Geneva, Switzerland.

World Health Organization (2017), *Vaccine Management Handbook: How to Calculate Vaccine Volumes and Cold Chain Capacity Requirements*, World Health Organization, Geneva.

World Health Organization (2021a), *Training on Handling, Storing and Transporting Pfizer BioNTech COVID-19 Vaccine COMIRNATY® (Tozinameran)*, World Health Organization, Geneva.

World Health Organization (2021b), *Guide to the Global WHO Vaccine Wastage Rates Calculator*, World Health Organization, Geneva.

World Health Organization (2024a), available at:, available at: https://who.int/emergencies/emergency-events/item (accessed 22 October 2024).

World Health Organization (2024b), E003 Refrigerators and Freezers, World Health Organization, Geneva.

World Health Organization (2025), *Vaccine Wastage Rates Calculator*, World Health Organization, Geneva.

World Health Organization (2026), "E002: refrigerated vehicles | WHO – Prequalification of medical products (IVDs, medicines, vaccines and immunization devices, vector control)", available at: https://extranet.who.int/prequal/immunization-devices/e002-refrigerated-vehicles (accessed 1 July 2026).

Yang, Y. and Rajgopal, J. (2021), "Outreach strategies for vaccine distribution: a multi-period stochastic modeling approach", *Operations Research Forum*, Vol. 2 No. 2, pp. 1-26.

Yang, Y., Bidkhori, H. and Rajgopal, J. (2021), "Optimizing vaccine distribution networks in low and middle-income countries", *Omega*, Vol. 99, p. 102197.

Zhao, H., Merchant, N.N., McNulty, A., Radcliff, T.A., Cote, M.J., Fischer, R.S.B., Sang, H. and Ory, M.G. (2021), "COVID-19: short term prediction model using daily incidence data", *PloS One*, Vol. 16 No. 4, p. e0250110.

Further reading

Mamani, H., Chick, S.E. and Simchi-Levi, D. (2013), "A game-theoretic model of international influenza vaccination coordination", *Management Science*, Vol. 59 No. 7, pp. 1650-1670, doi: 10.1287/MNSC.1120.1661.

Supplementary material

The supplementary material for this article can be found online.

Corresponding author

Sara Aryaee can be contacted at: sara.aryaee@ut.ac.ir

For instructions on how to order reprints of this article, please visit our website:
www.emeraldgrouppublishing.com/licensing/reprints.htm
Or contact us for further details: **permissions@emeraldinsight.com**

Downloaded from www.emerald.com/jhlscm/article-pdf/doi/10.1108/JHLSCM-11-2025-0229/11895066/jhlscm-11-2025-0229en.pdf by University of Sheffield user on 29 October 2026